CHAPTER 9

VISCOUS FLOW ALONG A WALL

9.1 THE NO-SLIP CONDITION

All liquids and gases are viscous and, as a consequence, a fluid near a solid boundary sticks to the boundary. The tendency for a liquid or gas to stick to a wall arises from momentum exchanged during molecular collisions with the wall. Viscous friction profoundly changes the fluid flow over a body compared to the ideal inviscid approximation that is widely applied in aerodynamic theory. The figure below illustrates the effect in the flow over a curved boundary. Later we will see how the velocity U_e at the wall from irrotational flow theory is used as the outer boundary condition for the equations that govern the thin region of rotational flow near the wall imposed by the no-slip condition. This thin layer is called a boundary layer.

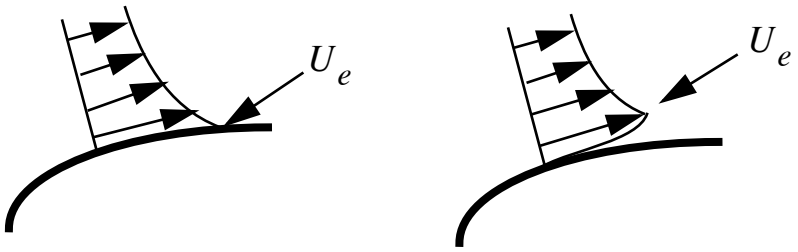

Figure 9.1 Slip versus no-slip flow near a solid surface.

The presence of low speed flow near the surface of a wing can lead to flow separation or stall. Separation can produce large changes in the pressure field surrounding the body leading to a decrease in lift and an increase in pressure related drag. The pressure drag due to stall may be much larger than the drag due to skin friction. In a supersonic flow the no-slip condition insures that there is always a subsonic flow near the wall enabling pressure disturbances to propagate upstream through the boundary layer. This may cause flow separation and shock formation leading to increased wave drag.

In Appendix 1 we worked out the mean free path between collisions in a gas

$$\lambda = \frac{1}{\sqrt{2}\pi n \sigma^2} \tag{9.1}$$

where n is the number of molecules per unit volume and σ is the collision diameter of the molecule. On an atomic scale all solid materials are rough and adsorb or retard gas molecules near the surface. When a gas molecule collides with a solid surface a certain fraction of its momentum parallel to the surface is lost due to Van der Walls forces and interpenetration of electron clouds with the molecules at the solid surface. Collisions of a rebounding gas molecule with other gas molecules within a few mean free paths of the surface will slow those molecules and cause the original molecule to collide multiple times with the surface. Within a few collision times further loss of tangential momentum will drop the average molecular velocity to zero. At equilibrium, the velocity of the gas within a small fraction of a mean free path of the surface and the velocity of the surface must match.

The exception to this occurs in the flow of a rarified gas where the distance a molecule travels after a collision with the surface is so large that a return to the surface may never occur and equilibrium is never established. In this case there is a slip velocity that can be modeled as

$$v_{slip} = C\lambda \frac{\partial U}{\partial y} \tag{9.2}$$

where C is a constant of order one. The slip velocity is negligible for typical values of the mean free path in gases of ordinary density. In situations where the velocity gradient is extremely large as in some gas lubrication flows there can be significant slip even at ordinary densities.

For similar reasons there can be a discontinuity in temperature between the wall and gas in rarified flows or very high shear rate flows.

In this Chapter we will discuss two fundamental problems involving viscous flow along a wall at ordinary density and shear rate. The first is plane Couette flow between two parallel plates where the flow is perfectly parallel. This problem can be solved exactly. The second is the plane boundary layer along a wall where the flow is almost but not quite perfectly parallel. In this case an approximate solution to the equations of motion can be determined.

9.2 EQUATIONS OF MOTION

Recall the equations of motion in Cartesian coordinates from Chapter 1, in the absence of body forces and internal sources of energy.

Conservation of mass

$$\frac{\partial \rho}{\partial t} + \frac{\partial \rho U}{\partial x} + \frac{\partial \rho V}{\partial y} + \frac{\partial \rho W}{\partial z} = 0$$

Conservation of momentum

$$\begin{aligned}
&\frac{\partial \rho U}{\partial t} + \frac{\partial (\rho UU + P - \tau_{xx})}{\partial x} + \frac{\partial (\rho UV - \tau_{xy})}{\partial y} + \frac{\partial (\rho UW - \tau_{xz})}{\partial z} = 0 \\
&\frac{\partial \rho V}{\partial t} + \frac{\partial (\rho VU - \tau_{xy})}{\partial x} + \frac{\partial (\rho VV + P - \tau_{yy})}{\partial y} + \frac{\partial (\rho VW - \tau_{yz})}{\partial z} = 0 \\
&\cdot\frac{\partial \rho W}{\partial t} + \frac{\partial (\rho WU - \tau_{xz})}{\partial x} + \frac{\partial (\rho WV - \tau_{yz})}{\partial y} + \frac{\partial (\rho WW + P - \tau_{zz})}{\partial z} = 0 .
\end{aligned} \tag{9.3}$$

Conservation of energy

$$\begin{aligned}
&\frac{\partial \rho e}{\partial t} + \frac{\partial (\rho hU + Q_x)}{\partial x} + \frac{\partial (\rho hV + Q_y)}{\partial y} + \frac{\partial (\rho hW + Q_z)}{\partial z} - \\
&\left(U\frac{\partial P}{\partial x} + V\frac{\partial P}{\partial y} + W\frac{\partial P}{\partial z}\right) - \left(\tau_{xx}\frac{\partial U}{\partial x} + \tau_{xy}\frac{\partial U}{\partial y} + \tau_{xz}\frac{\partial U}{\partial z}\right) - \\
&\left(\tau_{xy}\frac{\partial V}{\partial x} + \tau_{yy}\frac{\partial V}{\partial y} + \tau_{yz}\frac{\partial V}{\partial z}\right) - \left(\tau_{xz}\frac{\partial W}{\partial x} + \tau_{yz}\frac{\partial W}{\partial y} + \tau_{zz}\frac{\partial W}{\partial z}\right) = 0
\end{aligned}$$

The first simplification is to reduce the problem to steady flow in two space dimensions.

$$
\begin{aligned}
&\frac{\partial \rho U}{\partial x} + \frac{\partial \rho V}{\partial y} = 0 \\
&\frac{\partial(\rho UU + P - \tau_{xx})}{\partial x} + \frac{\partial(\rho UV - \tau_{xy})}{\partial y} = 0 \\
&\frac{\partial(\rho VU - \tau_{xy})}{\partial x} + \frac{\partial(\rho VV + P - \tau_{yy})}{\partial y} = 0 \\
&\frac{\partial(\rho hU + Q_x)}{\partial x} + \frac{\partial(\rho hV + Q_y)}{\partial y} - \left(U\frac{\partial P}{\partial x} + V\frac{\partial P}{\partial y}\right) \\
&-\left(\tau_{xx}\frac{\partial U}{\partial x} + \tau_{xy}\frac{\partial U}{\partial y}\right) - \left(\tau_{xy}\frac{\partial V}{\partial x} + \tau_{yy}\frac{\partial V}{\partial y}\right) = 0
\end{aligned}
\tag{9.4}
$$

9.3 PLANE, COMPRESSIBLE, COUETTE FLOW

First let's study the two-dimensional, compressible flow produced between two parallel plates in relative motion shown below. This is the simplest possible compressible flow where viscous forces and heat conduction dominate the motion. We studied the incompressible version of this flow in Chapter 1. There the gas temperature is constant and the velocity profile is a straight line. In the compressible problem the temperature varies substantially, as does the gas viscosity, leading to a more complex and more interesting problem.

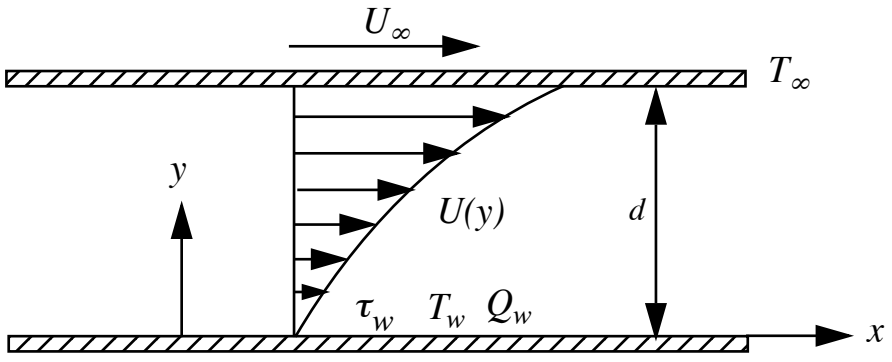

Figure 9.2 Flow produced between two parallel plates in relative motion

The upper wall moves at a velocity U_∞ doing work on the fluid while the lower wall is at rest. The temperature of the upper wall is T_∞. The flow is assumed to be steady with no variation in the z direction. The plates extend to plus and minus infinity in the x direction.

All gradients in the x direction are zero and the velocity in the y direction is zero.

$$\begin{aligned} V &= W = 0 \\ \frac{\partial}{\partial x}(\ ) &= \frac{\partial}{\partial z}(\ ) = 0 \end{aligned} \tag{9.5}$$

With these simplifications the equations of motion simplify to

$$\begin{aligned} \frac{\partial \tau_{xy}}{\partial y} &= 0 \\ \frac{\partial P}{\partial y} &= 0 \\ \frac{\partial (Q_y - \tau_{xy} U)}{\partial y} &= 0 \end{aligned} \quad . \tag{9.6}$$

The U velocity component and temperature only depend on y. The y momentum equation implies that the pressure is uniform throughout the flow (the pressure does not depend on x or y). The implication of the x momentum balance is that the shear stress τ_{xy} also must be uniform throughout the flow just like the pressure. Assume the fluid is Newtonian. With $V = 0$, the shear stress is

$$\tau_{xy} = \mu \frac{dU}{dy} = \tau_w = constant \tag{9.7}$$

where τ_w is the shear stress at the lower wall. For gases the viscosity depends only on temperature.

$$\mu = \mu(T) \tag{9.8}$$

Since the pressure is constant the density also depends only on the temperature. According to the perfect gas law

$$\rho(y) = \frac{P}{RT(y)}. \tag{9.9}$$

Using these equations, the solution for the velocity profile can be written as an integral.

$$U(y) = \tau_w \int_0^y \frac{dy}{\mu(T)} \tag{9.10}$$

To determine the velocity profile we need to know how the viscosity depends on temperature and the temperature distribution.

The temperature distribution across the channel can be determined from the energy equation. Fourier's law for the heat flux is

$$Q_y = -\kappa \frac{dT}{dy}. \tag{9.11}$$

The coefficient of heat conductivity, like the viscosity is also only a function of temperature.

$$\kappa = \kappa(T) \tag{9.12}$$

The relative rates of diffusion of momentum and heat are characterized by the Prandtl number.

$$P_r = \frac{C_p \mu}{\kappa} \tag{9.13}$$

In gases, heat and momentum are transported by the same mechanism of molecular collisions. For this reason the temperature dependencies of the viscosity and heat conductivity approximately cancel in (9.13). The heat capacity is only weakly dependent on temperature and so to a reasonable approximation the Prandtl number for gases tends to be a constant close to one. For Air $P_r = 0.71$.

9.3.1 The energy integral in plane Couette flow

The energy equation expresses the balance between heat flux and work done on the gas.

$$\frac{d}{dy}(-Q_y + \tau_w U) = 0. \tag{9.14}$$

Integrate (9.14).

$$-Q_y + \tau_w U = -Q_w \tag{9.15}$$

The constant of integration, $Q_w = \kappa(\partial T/\partial y)_{y=0}$, is the heat flux on the lower wall. Now insert the expressions for the shear stress and heat flux into (9.15).

$$k\frac{dT}{dy} + \mu U\frac{dU}{dy} = \mu\frac{d}{dy}\left(\frac{1}{Pr}C_p T + \frac{1}{2}U^2\right) = -Q_w \tag{9.16}$$

Integrate (9.16) from the lower wall.

$$C_p(T - T_w) + \frac{1}{2}P_r U^2 = -Q_w P_r \int_0^y \frac{dy}{\mu(T)} \tag{9.17}$$

T_w is the temperature of the lower wall. The integral on the right of (9.17) can be replaced by the velocity using (9.10). The result is the so-called *energy integral*.

$$C_p(T - T_w) + \frac{1}{2}P_r U^2 = -\frac{Q_w}{\tau_w}P_r U \tag{9.18}$$

At the upper wall, the temperature is T_∞ and this can now be used to evaluate the lower wall temperature.

$$C_p T_w = C_p T_\infty + P_r\left(\frac{U_\infty{}^2}{2} + \frac{Q_w}{\tau_w}U_\infty\right) \tag{9.19}$$

9.3.2 THE ADIABATIC WALL RECOVERY TEMPERATURE

Suppose the lower wall is insulated so that $Q_w = 0$. What temperature does the lower wall reach? This is called the adiabatic wall recovery temperature T_{wa}.

$$T_{wa} = T_\infty + \frac{P_r}{2C_p}U_\infty{}^2 \tag{9.20}$$

Introduce the Mach number $M_\infty = U_\infty/a_\infty$. Now

$$\frac{T_{wa}}{T_\infty} = 1 + P_r\left(\frac{\gamma - 1}{2}\right) M_\infty{}^2 . \tag{9.21}$$

Equation (9.21) indicates that the recovery temperature equals the stagnation temperature at the upper wall only for a Prandtl number of one. The stagnation temperature at the upper wall is

$$\frac{T_{t_\infty}}{T_\infty} = 1 + \left(\frac{\gamma - 1}{2}\right) M_\infty{}^2 . \tag{9.22}$$

The recovery factor is defined as

$$\frac{T_{wa} - T_\infty}{T_{t_\infty} - T_\infty} = r . \tag{9.23}$$

In Couette flow for a perfect gas with constant C_p (9.21) tells us that the recovery factor is the Prandtl number.

$$\frac{T_{wa} - T_\infty}{T_{t_\infty} - T_\infty} = P_r \tag{9.24}$$

Equations (9.19) and (9.20) can be used to show that the heat transfer and shear stress are related by

$$\frac{Q_w}{\tau_w U_\infty} = \frac{C_p(T_w - T_{wa})}{P_r U_\infty^2} . \tag{9.25}$$

Equation (9.25) can be rearranged to read

$$\frac{\tau_w}{\frac{1}{2}\rho_\infty U_\infty^2} = 2P_r\left(\frac{Q_w}{\rho_\infty U_\infty C_p(T_w - T_{wa})}\right) . \tag{9.26}$$

The left side of (9.26) is the friction coefficient

$$C_f = \frac{\tau_w}{\frac{1}{2}\rho_\infty U_\infty^2} . \tag{9.27}$$

On the right side of (9.26) there appears a dimensionless heat transfer coefficient called the Stanton number.

$$S_t = \frac{Q_w}{\rho_\infty U_\infty C_p (T_w - T_{wa})} \tag{9.28}$$

In order to transfer heat into the fluid the lower wall temperature must exceed the recovery temperature. Equation (9.26) now becomes

$$C_f = 2 P_r S_t . \tag{9.29}$$

The coupling between heat transfer and viscous friction indicated in (9.29) is a general property of all compressible flows near a wall. The numerical factor 2 may change and the dependence on Prandtl number may change depending on the flow geometry and on whether the flow is laminar or turbulent, but the general property that heat transfer affects the viscous friction is universal.

9.3.3 Velocity distribution in Couette flow

Now that the relation between temperature and velocity is known we can integrate the momentum relation for the stress. We use the energy integral written in terms of T_∞

$$C_p (T - T_\infty) = P_r \frac{Q_w}{\tau_w} (U_\infty - U) + \frac{1}{2} P_r (U_\infty{}^2 - U^2) \tag{9.30}$$

or

$$\frac{T}{T_\infty} = 1 + P_r \frac{Q_w}{U_\infty \tau_w} (\gamma - 1) M_\infty^2 \left(1 - \frac{U}{U_\infty}\right) + P_r \left(\frac{\gamma - 1}{2}\right) M_\infty^2 \left(1 - \frac{U^2}{U_\infty{}^2}\right). \tag{9.31}$$

Recall the momentum equation.

$$\mu(T) \frac{dU}{dy} = \tau_w \tag{9.32}$$

The temperature is a monotonic function of the velocity and so the viscosity can be regarded as a function of U. This enables the momentum equation to be integrated.

$$\int_0^U \mu(U)dU \;=\; \tau_w y \tag{9.33}$$

In gases, the dependence of viscosity on temperature is reasonably well approximated by Sutherland's law.

$$\frac{\mu}{\mu_\infty} \;=\; \left(\frac{T}{T_\infty}\right)^{3/2}\left(\frac{T_\infty + T_S}{T + T_S}\right) \tag{9.34}$$

where T_S is the Sutherland reference temperature which is $110.4K$ for Air. An approximation that is often used is the power law.

$$\frac{\mu}{\mu_\infty} \;=\; \left(\frac{T}{T_\infty}\right)^{\omega} \qquad 0.5 < \omega < 1.0 \tag{9.35}$$

Using (9.31) and (9.35), the momentum equation becomes

$$\int_0^U \left(1 + P_r\frac{Q_w}{U_\infty \tau_w}(\gamma-1)M_\infty^2\left(1-\frac{U}{U_\infty}\right) + P_r\left(\frac{\gamma-1}{2}\right)M_\infty^2\left(1-\frac{U^2}{U_\infty{}^2}\right)\right)^{\omega} dU \;=\; \frac{\tau_w}{\mu_\infty} y \tag{9.36}$$

For Air the exponent, ω, is approximately 0.76. The simplest case, and a reasonable approximation, corresponds to $\omega = 1$. In this case the integral can be carried out explicitly. For an adiabatic wall, $Q_w = 0$ the wall stress and velocity are related by

$$\frac{\tau_w}{\mu_\infty U_\infty} y \;=\; \frac{U}{U_\infty} + P_r\left(\frac{\gamma-1}{2}\right)M_\infty^2\left(\frac{U}{U_\infty} - \frac{1}{3}\left(\frac{U}{U_\infty}\right)^3\right). \tag{9.37}$$

The shear stress is determined by evaluating (9.37) at the upper wall.

$$\frac{\tau_w}{\mu_\infty U_\infty} d \;=\; 1 + P_r\left(\frac{\gamma-1}{3}\right)M_\infty^2 \tag{9.38}$$

The velocity profile is expressed implicitly as

$$\frac{y}{d} = \frac{\frac{U}{U_\infty} + P_r\left(\frac{\gamma - 1}{2}\right) M_\infty^2 \left(\frac{U}{U_\infty} - \frac{1}{3}\left(\frac{U}{U_\infty}\right)^3\right)}{1 + P_r\left(\frac{\gamma - 1}{3}\right) M_\infty^2} . \tag{9.39}$$

At $M_\infty \to 0$ the profile reduces to the incompressible limit $U/U_\infty = y/d$. At high Mach number the profile is

$$\lim_{M_\infty \to \infty}\left(\frac{y}{d}\right) = \left(\frac{3}{2}\right)\left(\frac{U}{U_\infty} - \frac{1}{3}\left(\frac{U}{U_\infty}\right)^3\right) . \tag{9.40}$$

At high Mach number the profile is independent of the Prandtl number and Mach number. The two limiting cases are shown below.

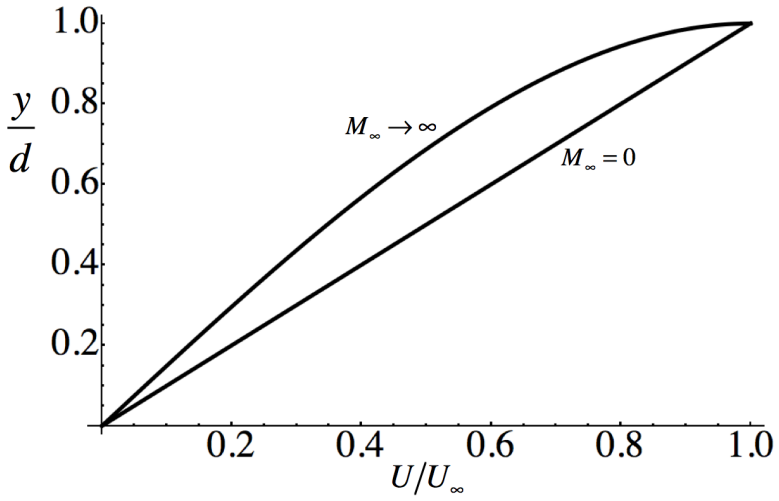

Figure 9.3 Velocity distribution in plane Couette flow for an adiabatic lower wall and $\omega = 1$.

Using (9.38) the wall friction coefficient for an adiabatic lower wall is expressed in terms of the Prandtl, Reynolds and Mach numbers.

$$C_f = 2\left(\frac{1 + P_r\left(\frac{\gamma - 1}{3}\right) M_\infty^2}{R_e}\right) \tag{9.41}$$

where the Reynolds number is

$$R_e = \frac{\rho_\infty U_\infty d}{\mu_\infty} \tag{9.42}$$

The Reynolds number can be expressed as

$$R_e = \frac{\rho_\infty U_\infty d}{\mu_\infty} = \frac{\frac{1}{2}\rho_\infty U_\infty^2}{\frac{1}{2}\mu_\infty \frac{U_\infty}{d}} = \frac{\textit{dynamic pressure at the upper plate}}{\textit{characteristic shear stress}}. \tag{9.43}$$

Here the interpretation of the Reynolds number as a ratio of convective to viscous forces is nicely illustrated.

Notice that if the upper and lower walls are both adiabatic the work done by the upper wall would lead to a continuous accumulation of energy between the two plates and a continuous rise in temperature. In this case a steady state solution to the problem would not exist. The upper wall has to be able to conduct heat into or out of the flow for a steady state solution to be possible.

9.4 THE VISCOUS BOUNDARY LAYER ON A WALL

The Couette problem provides a useful insight into the nature of compressible flow near a solid boundary. From a practical standpoint the more important problem is that of a compressible boundary layer where the flow originates at the leading edge of a solid body such as an airfoil. A key reference is the classic text *Boundary Layer Theory* by Hermann Schlichting. Recent editions are authored by Schlichting and Gersten.

To introduce the boundary layer concept we will begin by considering viscous, compressible flow past a flat plate of length L shown in Figure 9.4. The question of whether a boundary layer is present or not depends on the overall Reynolds number of the flow.

$$R_{eL} = \frac{\rho_\infty U_\infty L}{\mu_\infty} \tag{9.44}$$

Figure 9.4 depicts the case where the thickness of the viscous region, delineated, schematically by the parabolic boundary, is a significant fraction of the length of the plate and the Reynolds number based on the plate length is quite low.

In this case there is no boundary layer and the full equations of motion must be solved to determine the flow.

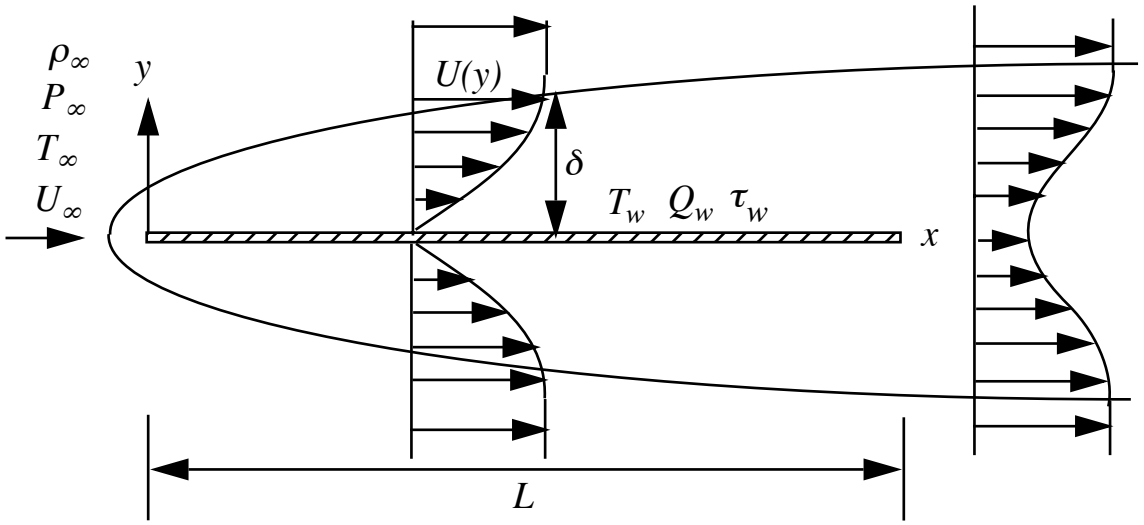

Figure 9.4 Low Reynolds number flow about a thin flat plate of length L. R_{eL} is less than a hundred or so. The parabolic envelope which extends upstream of the leading edge roughly delineates the region of rotational flow produced as a consequence of the no slip condition on the plate.

If the Reynolds number based on plate length is large then the flow looks more like that depicted in Figure 9.5.

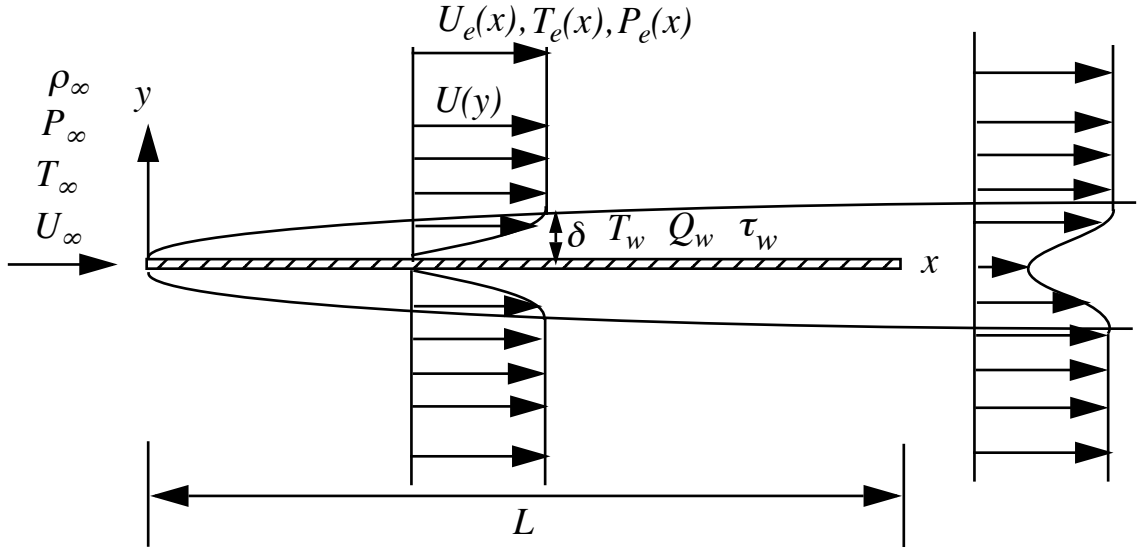

Figure 9.5 High Reynolds number flow developing from the leading edge of a flat plate of length L. R_{eL} is several hundred or more.

At high Reynolds number the thickness of the viscous region is much less than the length of the plate.

$$\frac{\delta}{L} \ll 1 \tag{9.45}$$

Moreover, there is a region of the flow away from the leading and trailing edges of the plate where the guiding effect of the plate produces a flow that is nearly parallel. In this region the transverse velocity component is much less than the streamwise component.

$$\frac{V}{U} \ll 1 \tag{9.46}$$

The variation of the flow in the streamwise direction is much smaller than the variation in the cross-stream direction. Thus

$$\frac{\partial(\ )}{\partial x} \ll \frac{\partial(\ )}{\partial y} \qquad U\frac{\partial(\ )}{\partial x} \sim V\frac{\partial(\ )}{\partial y}. \tag{9.47}$$

Moreover continuity tells us that

$$\frac{\partial U}{\partial x} \sim -\frac{\partial V}{\partial y}. \tag{9.48}$$

The convective and viscous terms in the streamwise momentum equation are of the same order suggesting the following estimate for δ/L.

$$\frac{\rho_\infty {U_\infty}^2}{L} \approx \mu\frac{U_\infty}{\delta^2} \Rightarrow \frac{\delta}{L} \approx \frac{1}{(R_{eL})^{1/2}} \tag{9.49}$$

With this estimate in mind let's examine the y momentum equation.

$$\frac{\partial(\rho VU - \tau_{xy})}{\partial x} + \frac{\partial(\rho VV + P - \tau_{yy})}{\partial y} = 0 \tag{9.50}$$

Utilizing (9.46) and (9.47), equation (9.50) reduces to

$$\frac{\partial(P - \tau_{yy})}{\partial y} = 0. \tag{9.51}$$

Now integrate this equation at a fixed position x and evaluate the constant of integration in the free stream.

$$P(x, y) = \tau_{yy}(x, y) + P_e(x) \tag{9.52}$$

The pressure (9.52) is inserted into the x momentum equation in (9.4). The result is the boundary layer approximation to the x momentum equation.

$$\rho U\frac{\partial U}{\partial x} + \rho V\frac{\partial U}{\partial y} = -\frac{dP_e}{dx} + \frac{\partial}{\partial x}(\tau_{xx} - \tau_{yy}) + \frac{\partial \tau_{xy}}{\partial y} \tag{9.53}$$

Now consider the energy equation.

$$\begin{gathered}\frac{\partial(\rho hU + Q_x)}{\partial x} + \frac{\partial(\rho hV + Q_y)}{\partial y} - \\ \left(U\frac{\partial P}{\partial x} + V\frac{\partial P}{\partial y}\right) - \left(\tau_{xx}\frac{\partial U}{\partial x} + \tau_{xy}\frac{\partial U}{\partial y}\right) - \\ \left(\tau_{xy}\frac{\partial V}{\partial x} + \tau_{yy}\frac{\partial V}{\partial y}\right) = 0\end{gathered} \tag{9.54}$$

Using (9.46), (9.47) and (9.48) the energy equation simplifies to

$$\begin{gathered}\rho U\frac{\partial h}{\partial x} + \rho V\frac{\partial h}{\partial y} + \frac{\partial Q_y}{\partial y} - U\frac{dP_e}{dx} + U\frac{\partial}{\partial x}(\tau_{xx} - \tau_{yy}) - \\ \frac{\partial(V\tau_{yy})}{\partial y} - \frac{\partial(U\tau_{xx})}{\partial x} - \tau_{xy}\frac{\partial U}{\partial y} = 0\end{gathered} \tag{9.55}$$

In laminar flow the normal stresses τ_{xx} and τ_{yy} are very small and the normal stress terms that appear in (9.53) and (9.55) can be neglected. In turbulent flow the normal stresses are not particularly small, with fluctuations of velocity near the wall that can be *10 – 20* percent of the velocity at the edge of the boundary layer. Nevertheless a couple of features of the turbulent boundary layer (compressible or incompressible) allow these normal stress terms in the boundary layer equations to be neglected.

1) τ_{xx} and τ_{yy} tend to be comparable in magnitude so that $\tau_{xx} - \tau_{yy}$ is small and the streamwise derivative $\partial(\tau_{xx} - \tau_{yy})/\partial x$ is generally quite small.

2) τ_{yy} has its maximum value in the lower part of the boundary layer where V is very small so the product $V\tau_{yy}$ is small.

3) τ_{xx} also has its maximum value relatively near the wall where U is relatively small and the streamwise derivative of $U\tau_{xx}$ is small.

Using these assumptions to remove the normal stress terms, the compressible boundary layer equations become

$$\frac{\partial \rho U}{\partial x} + \frac{\partial \rho V}{\partial y} = 0$$

$$\rho U\frac{\partial U}{\partial x} + \rho V\frac{\partial U}{\partial y} = -\frac{dP_e}{dx} + \frac{\partial \tau_{xy}}{\partial y} \qquad . \tag{9.56}$$

$$\rho U\frac{\partial h}{\partial x} + \rho V\frac{\partial h}{\partial y} + \frac{\partial Q_y}{\partial y} - U\frac{dP_e}{dx} - \tau_{xy}\frac{\partial U}{\partial y} = 0$$

The only stress component that plays a role in this approximation is the shearing stress τ_{xy}. In a turbulent boundary layer both the laminar and turbulent shearing stresses are important.

$$\tau_{xy} = \tau_{xy}\Big|_{laminar} + \tau_{xy}\Big|_{turbulent} = \mu\frac{\partial U}{\partial y} + \tau_{xy}\Big|_{turbulent} \tag{9.57}$$

In the outer part of the layer where the velocity gradient is relatively small the turbulent stresses dominate, but near the wall where the velocity fluctuations are damped and the velocity gradient is large, the viscous stress dominates.

The flow picture appropriate to the boundary layer approximation is shown below.

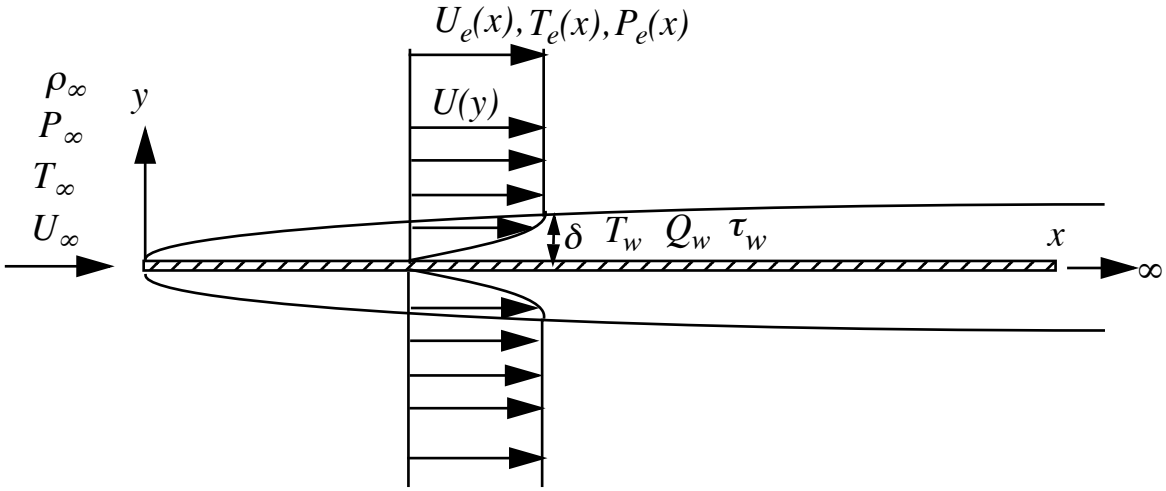

Figure 9.6 High Reynolds number flow developing from the leading edge of a semi-infinite flat plate.

The boundary layer is assumed to originate from a virtual origin near the plate leading edge and the wake is infinitely far off to the right. The velocity, temperature and pressure at the boundary layer edge are assumed to be known functions. The appropriate measure of the Reynolds number in this flow is based on the distance from the leading edge.

$$R_{ex} = \frac{\rho_\infty U_\infty x}{\mu_\infty} \tag{9.58}$$

One would expect a thin flat plate to produce very little disturbance to the flow. So it is a bit hard at this point to see the origin of the variation in free stream velocity indicated in Figure 9.6 . We will return to this question at the end of the chapter. For now we simply accept that the free stream pressure and velocity can vary with x even along a thin flat plate. By the way, an experimental method for generating a pressure gradient is to put the plate into a wind tunnel with variable walls that can be set at an angle to accelerate or decelerate the flow.

For Newtonian laminar flow the stress is

$$\tau_{ij} = 2\mu S_{ij} - \left(\frac{2}{3}\mu - \mu_v\right)\delta_{ij}S_{kk}$$
$$\tau_{xy} = \mu\left(\frac{\partial U}{\partial y} + \frac{\partial V}{\partial x}\right) \cong \mu\frac{\partial U}{\partial y} \quad . \tag{9.59}$$

The diffusion of heat is governed by Fourier's law introduced earlier.

$$Q_y = -\kappa\frac{\partial T}{\partial y} \tag{9.60}$$

For laminar flow the compressible boundary layer equations are

$$\frac{\partial \rho U}{\partial x} + \frac{\partial \rho V}{\partial y} = 0$$
$$\rho U\frac{\partial U}{\partial x} + \rho V\frac{\partial U}{\partial y} = -\frac{dP_e}{dx} + \frac{\partial}{\partial y}\left(\mu\frac{\partial U}{\partial y}\right) \quad . \tag{9.61}$$
$$\rho U C_p\frac{\partial T}{\partial x} + \rho V C_p\frac{\partial T}{\partial y} = U\frac{dP_e}{dx} + \frac{\partial}{\partial y}\left(\kappa\frac{\partial T}{\partial y}\right) + \mu\left(\frac{\partial U}{\partial y}\right)^2$$

9.4.1 Measures of boundary layer thickness

The thickness of the boundary layer depicted in Figure 9.6 is denoted by δ. There are several ways to define the thickness. The simplest is to identify the point where the velocity is some percentage of the free stream value, say $\delta_{0.95}$ or $\delta_{0.99}$. More rigorous and in some ways more useful definitions are the following.

Displacement thickness

$$\delta^* = \int_0^\delta \left(1 - \frac{\rho U}{\rho_e U_e}\right) dy \tag{9.62}$$

This is a measure of the distance by which streamlines are shifted away from the plate by the blocking effect of the boundary layer. This outward displacement of the flow comes from the reduced mass flux in the boundary layer compared to the mass flux that would occur if the flow were inviscid. Generally δ^* is a fraction of $\delta_{0.99}$. The integral (9.62) is terminated at the edge of the boundary layer where

the velocity equals the free stream value U_e. This is important in a situation involving a pressure gradient where the velocity profile might look something like that depicted in Figure 9.1. The free stream velocity used as the outer boundary condition for the boundary layer calculation comes from the potential flow solution for the irrotational flow about the body evaluated at the wall. If the integral (9.62) is taken beyond this point it will begin to diverge.

Momentum thickness

$$\theta = \int_0^{\delta} \frac{\rho U}{\rho_e U_e}\left(1 - \frac{U}{U_e}\right) dy \tag{9.63}$$

This is a measure of the deficit in momentum flux within the boundary layer compared to the free stream value and is smaller than the displacement thickness. The evolution of the momentum thickness along the wall is directly related to the skin friction coefficient.

9.5 THE VON KARMAN INTEGRAL MOMENTUM EQUATION

Often the detailed structure of the boundary layer velocity profile is not the primary object of interest. The most important properties of the boundary layer are the skin friction and displacement effect. Boundary layer models often focus primarily on these variables.

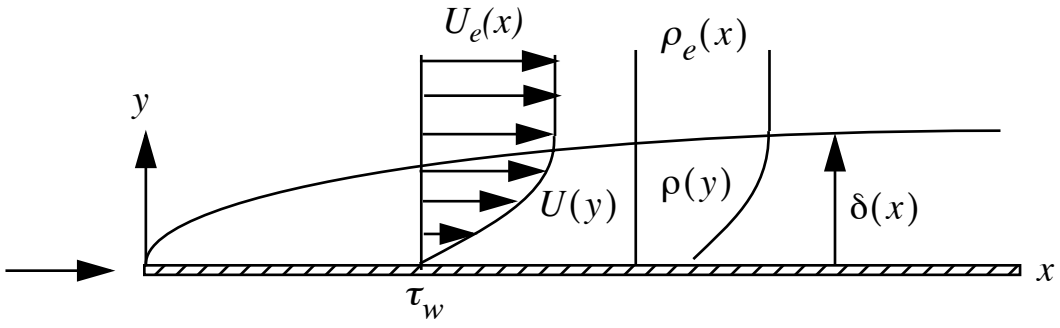

Figure 9.7 Boundary layer velocity and density profiles.

The steady compressible boundary layer equations (9.53) and (9.55) together with the continuity equation are repeated her for convenience.

$$\begin{aligned} \frac{\partial \rho U}{\partial x} + \frac{\partial \rho V}{\partial y} &= 0 \\ \frac{\partial \rho U^2}{\partial x} + \frac{\partial \rho UV}{\partial y} &= -\frac{dP_e}{dx} + \frac{\partial \tau_{xy}}{\partial y} \end{aligned} \tag{9.64}$$

Integrate the continuity and momentum equations over the thickness of the boundary layer.

$$\begin{aligned} \int_0^{\delta(x)} \left(\frac{\partial \rho U}{\partial x}\right) dy + \int_0^{\delta(x)} \left(\frac{\partial \rho V}{\partial y}\right) dy &= 0 \\ \int_0^{\delta(x)} \left(\frac{\partial \rho U^2}{\partial x}\right) dy + \int_0^{\delta(x)} \left(\frac{\partial \rho UV}{\partial y}\right) dy &= -\int_0^{\delta(x)} \left(\frac{dP_e}{dx}\right) dy + \int_0^{\delta(x)} \left(\frac{\partial \tau_{xy}}{\partial y}\right) dy \end{aligned} \tag{9.65}$$

Upon integration the momentum equation becomes

$$\int_0^{\delta(x)} \left(\frac{\partial \rho U^2}{\partial x}\right) dy + \rho_e U_e V_e = -\left(\frac{dP_e}{dx}\right) \delta(x) + \tau_{xy}\Big|_{y=0} \tag{9.66}$$

The partial derivatives with respect to x in (9.64) can be taken outside the integral using Liebniz' rule.

$$\begin{aligned} \frac{d}{dx}\int_0^{\delta(x)} \rho U dy &= \int_0^{\delta(x)} \left(\frac{\partial \rho U}{\partial x}\right) dy + \rho_e U_e \frac{d\delta}{dx} \\ \frac{d}{dx}\int_0^{\delta(x)} \rho U^2 dy &= \int_0^{\delta(x)} \left(\frac{\partial \rho U^2}{\partial x}\right) dy + \rho_e U_e^2 \frac{d\delta}{dx} \end{aligned} \tag{9.67}$$

Use the second equation in (9.67) in (9.66).

$$\frac{d}{dx}\int_0^{\delta(x)} \rho U^2 dy - \rho_e U_e^2 \frac{d\delta}{dx} + \rho_e U_e V_e + \left(\frac{dP_e}{dx}\right) \delta(x) = -\tau_w \tag{9.68}$$

where $\tau_w(x) = -\tau_{xy}(x, 0)$ and τ_w is positive. We will make use of the following relation.

$$\frac{d}{dx}\int_0^{\delta(x)} \rho U U_e dy \;=\; \int_0^{\delta(x)} \left(\frac{\partial \rho U U_e}{\partial x}\right) dy + \rho_e U_e^2 \frac{d\delta}{dx} \;=$$

$$\int_0^{\delta(x)} \left(U_e \frac{\partial \rho U}{\partial x} + \rho U \frac{dU_e}{dx}\right) dy + \rho_e U_e^2 \frac{d\delta}{dx} \;= \tag{9.69}$$

$$U_e \int_0^{\delta(x)} \left(\frac{\partial \rho U}{\partial x}\right) dy + \frac{dU_e}{dx}\int_0^{\delta(x)} \rho U dy + \rho_e U_e^2 \frac{d\delta}{dx}$$

Multiply the continuity equation in (9.65) by U_e and integrate with respect to y.

$$U_e \int_0^{\delta(x)} \left(\frac{\partial \rho U}{\partial x}\right) dy + \rho_e U_e V_e \;=\; 0 \tag{9.70}$$

Insert (9.70) in the last relation in (9.69).

$$\frac{d}{dx}\int_0^{\delta(x)} \rho U U_e dy + \rho_e U_e V_e - \frac{dU_e}{dx}\int_0^{\delta(x)} \rho U dy - \rho_e U_e^2 \frac{d\delta}{dx} \;=\; 0 \tag{9.71}$$

Subtract(9.71) from (9.68).

$$\frac{d}{dx}\int_0^{\delta(x)} (\rho U^2 - \rho U U_e) dy + \frac{dU_e}{dx}\int_0^{\delta(x)} \rho U dy + \left(\frac{dP_e}{dx}\right)\delta(x) \;=\; -\tau_w \tag{9.72}$$

and subtract the identity

$$\frac{dU_e}{dx}\int_0^{\delta(x)} \rho_e U_e dy - \rho_e U_e \frac{dU_e}{dx}\delta(x) \;=\; 0 \tag{9.73}$$

from (9.72). Now the integral momentum equation takes the form

$$\frac{d}{dx}\int_0^{\delta(x)} (\rho U^2 - \rho U U_e) dy + \frac{dU_e}{dx}\int_0^{\delta(x)} (\rho U - \rho_e U_e) dy +$$

$$\left(\frac{dP_e}{dx} + \rho_e U_e \frac{dU_e}{dx}\right)\delta(x) \;=\; -\tau_w \tag{9.74}$$

Recall the definitions of displacement thickness (9.62) and momentum thickness (9.63).

$$\delta^*(x) = \int_0^{\delta(x)} \left(1 - \frac{\rho U}{\rho_e U_e}\right) dy$$
$$\theta(x) = \int_0^{\delta(x)} \frac{\rho U}{\rho_e U_e}\left(1 - \frac{U}{U_e}\right) dy \tag{9.75}$$

Substitute (9.75) into (9.74). The result is

$$\frac{d}{dx}(\rho_e U_e^2 \theta) + \rho_e U_e \delta^* \frac{dU_e}{dx} + \left(\frac{dP_e}{dx} + \rho_e U_e \frac{dU_e}{dx}\right) \delta(x) = \tau_w \tag{9.76}$$

At the edge of the boundary layer both $\partial U / \partial y$ and τ_{xy} go to zero and the x-boundary layer momentum equation reduces to the Euler equation.

$$dP_e + \rho_e U_e dU_e = 0 \tag{9.77}$$

Using (9.77), the integral equation (9.76) reduces to

$$\frac{d}{dx}(\rho_e U_e^2 \theta) + \rho_e U_e \delta^* \frac{dU_e}{dx} = \tau_w \tag{9.78}$$

The significance of this last step is that (9.78) does not depend explicitly on the percieved boundary layer thickness $\delta(x)$ but only on the more precisely defined momentum and displacement thicknesses. It is customary to write (9.78) in a slightly different form. Introduce the wall friction coefficient and carry out the differentiation of the first term in (9.78).

$$C_f = \frac{\tau_w}{\frac{1}{2}\rho_e U_e^2} \tag{9.79}$$

The Von Karman integral momentum equation is

$$\frac{d\theta}{dx} + (2\theta + \delta^*)\frac{1}{U_e}\frac{dU_e}{dx} = \frac{C_f}{2} \tag{9.80}$$

Another common form of (9.80) is generated by introducing the shape factor

$$H = \frac{\delta^*}{\theta} \tag{9.81}$$

and (9.80) becomes

$$\frac{d\theta}{dx} + (2 + H)\frac{\theta}{U_e}\frac{dU_e}{dx} = \frac{C_f}{2} \tag{9.82}$$

Equation (9.82) is valid for laminar, turbulent, compressible and incompressible flow.

9.6 THE LAMINAR BOUNDARY LAYER IN THE LIMIT $M^2 \to 0$

At very low Mach number the density, ρ is constant, temperature variations throughout the flow are very small and the boundary layer equations (9.61) reduce to their incompressible form.

$$\begin{aligned} \frac{\partial U}{\partial x} + \frac{\partial V}{\partial y} &= 0 \\ U\frac{\partial U}{\partial x} + V\frac{\partial U}{\partial y} &= -\frac{1}{\rho}\frac{dP_e}{dx} + \nu\left(\frac{\partial^2 U}{\partial y^2}\right) \end{aligned} \tag{9.83}$$

where the kinematic viscosity $\nu = \mu/\rho$ has been introduced. The boundary conditions are

$$U(0) = V(0) = 0 \qquad U(\delta) = U_e . \tag{9.84}$$

The pressure at the edge of the boundary layer $y = \delta$ is determined using the Bernoulli relation

$$P_t = P_e(x) + \frac{1}{2}\rho U_e(x)^2 \Rightarrow \frac{1}{\rho}\frac{dP_e}{dx} = -U_e\frac{dU_e}{dx} . \tag{9.85}$$

The stagnation pressure is constant in the irrotational flow outside the boundary layer. The pressure at the boundary layer edge, $P_e(x)$, is assumed to be a given function determined from a potential flow solution for the flow outside the boundary layer.

The continuity equation is satisfied identically by introducing a stream function.

$$U = \frac{\partial \psi}{\partial y} \qquad V = -\frac{\partial \psi}{\partial x} \tag{9.86}$$

In terms of the stream function, the governing momentum equation becomes a third-order partial differential equation.

$$\psi_y \psi_{xy} - \psi_x \psi_{yy} = U_e \frac{dU_e}{dx} + \nu \psi_{yyy} \tag{9.87}$$

9.6.1 THE ZERO PRESSURE GRADIENT, INCOMPRESSIBLE BOUNDARY LAYER

For $dU_e/dx = 0$ the governing equation reduces to

$$\psi_y \psi_{xy} - \psi_x \psi_{yy} = \nu \psi_{yyy}. \tag{9.88}$$

with boundary conditions

$$\psi(x, 0) = \psi_y(x, 0) = 0 \qquad \psi_y(x, \infty) = U_e \tag{9.89}$$

We can solve this problem using a symmetry arguement. Transform (9.88) using the following three parameter dilation Lie group.

$$\tilde{x} = e^a x \qquad \tilde{y} = e^b y \qquad \psi = e^c \psi \tag{9.90}$$

Equation (9.88) transforms as follows.

$$\tilde{\psi}_{\tilde{y}} \tilde{\psi}_{\tilde{x}\tilde{y}} - \tilde{\psi}_{\tilde{x}} \tilde{\psi}_{\tilde{y}\tilde{y}} - \nu \tilde{\psi}_{\tilde{y}\tilde{y}\tilde{y}} = e^{2c-a-2b}(\psi_y \psi_{xy} - \psi_x \psi_{yy}) - e^{c-3b}(\nu \tilde{\psi}_{\tilde{y}\tilde{y}\tilde{y}}) = 0 \tag{9.91}$$

Equation (9.88) is invariant under the group (9.90) if and only if $c = a - b$. The boundaries of the problem at the wall and at infinity are clearly invariant under (9.90).

$$\begin{aligned} \tilde{y} = e^b y = 0 &\Rightarrow y = 0 \\ \tilde{\psi}(\tilde{x}, 0) = e^c \psi(e^a x, 0) = 0 &\Rightarrow \psi(x, 0) = 0 \\ \tilde{\psi}_{\tilde{y}}(\tilde{x}, 0) = e^{c-b} \psi_y(e^a x, 0) = 0 &\Rightarrow \psi_y(x, 0) = 0 \end{aligned} \tag{9.92}$$

The free stream boundary condition requires some care.

$$\tilde{\psi}_{\tilde{y}}(\tilde{x}, \infty) = e^{c-b} \psi_y(e^a x, \infty) = U_e \tag{9.93}$$

Invariance of the free stream boundary condition only holds if $c = b$. So the problem as a whole, equation and boundary conditions, is invariant under the one-parameter group

$$\tilde{x} = e^{2b}x \qquad \tilde{y} = e^{b}y \qquad \psi = e^{b}\psi \tag{9.94}$$

This process of showing that the problem is invariant under a Lie group is essentially a proof of the existence of a similarity solution to the problem. We can expect that the solution of the problem will also be invariant under the same group (9.94). That is we can expect a solution of the form

$$\frac{\psi}{\sqrt{x}} = F\left(\frac{y}{\sqrt{x}}\right) \tag{9.95}$$

The problem can be further simplified by using the parameters of the problem to nondimensionalize the similarity variables. Introduce

$$\psi = (2\nu U_\infty x)^{1/2} F(\alpha) \qquad \alpha = y\left(\frac{U_\infty}{2\nu x}\right)^{1/2} \tag{9.96}$$

In terms of these variables the velocities are

$$\frac{U}{U_\infty} = F_\alpha \qquad \frac{V}{U_\infty} = \left(\frac{\nu}{2U_\infty x}\right)^{1/2}(\alpha F_\alpha - F)\ . \tag{9.97}$$

The Reynolds number in this flow is based on the distance from the leading edge, (9.58).

$$R_{ex} = \frac{U_\infty x}{\nu} \tag{9.98}$$

As the distance from the leading edge increases, the Reynolds number increases, V/U decreases, and the boundary layer approximation becomes more and more accurate. The vorticity in the boundary layer is

$$\omega = \frac{\partial V}{\partial x} - \frac{\partial U}{\partial y} \cong -U_\infty\left(\frac{U_\infty}{2\nu x}\right)^{1/2} F_{\alpha\alpha}. \tag{9.99}$$

The remaining derivatives that appear in (9.88) are

$$\psi_{xy} = -\frac{U_\infty}{2x}\alpha F_{\alpha\alpha}$$

$$\psi_{yy} = U_\infty\left(\frac{U_\infty}{2\nu x}\right)^{1/2} F_{\alpha\alpha}. \tag{9.100}$$

$$\psi_{yyy} = \frac{U_\infty^2}{2\nu x}F_{\alpha\alpha\alpha}$$

Substitute (9.97) and (9.100) into (9.88).

$$U_\infty F_\alpha\left(-\frac{U_\infty}{2x}\alpha F_{\alpha\alpha}\right) - U_\infty\left(\left(\frac{\nu}{2U_\infty x}\right)^{1/2}(\alpha F_\alpha - F)\right)U_\infty\left(\frac{U_\infty}{2\nu x}\right)^{1/2} F_{\alpha\alpha} = \nu\frac{U_\infty^2}{2\nu x}F_{\alpha\alpha\alpha} \tag{9.101}$$

$$-F_\alpha(\alpha F_{\alpha\alpha}) + (\alpha F_\alpha - F)F_{\alpha\alpha} = F_{\alpha\alpha\alpha}$$

$$-\alpha F_\alpha F_{\alpha\alpha} - FF_{\alpha\alpha} + \alpha F_\alpha F_{\alpha\alpha} - F_{\alpha\alpha\alpha} = 0$$

Canceling terms in (9.101) leads to the Blasius equation

$$F_{\alpha\alpha\alpha} + FF_{\alpha\alpha} = 0 \tag{9.102}$$

subject to the boundary conditions

$$F(0) = 0 \qquad F_\alpha(0) = 0 \qquad F_\alpha(\infty) = 1. \tag{9.103}$$

The numerical solution of the Blasius equation is shown below.

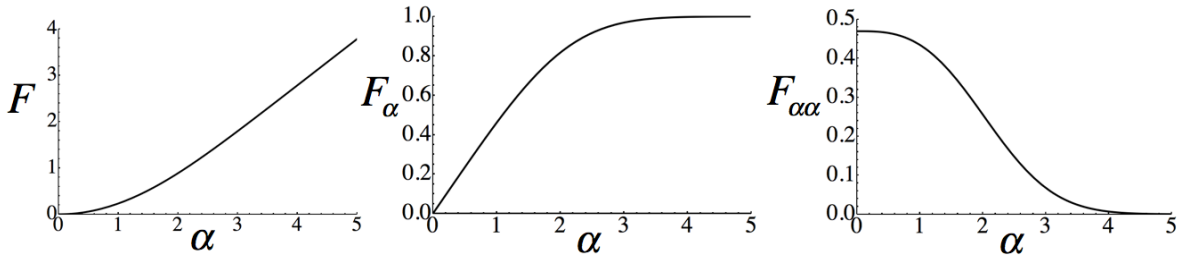

Figure 9.8 Solution of the Blasius equation (9.102) for the streamfunction, velocity and stress (or vorticity) profile in a zero pressure gradient laminar boundary layer.

The friction coefficient derived from evaluating the velocity gradient at the wall is

$$C_f = \frac{\tau_w}{(1/2)\rho U_\infty^2} = \frac{0.664}{\sqrt{R_{ex}}}. \tag{9.104}$$

The transverse velocity component at the edge of the layer is

$$\frac{V_e}{U_\infty} = \frac{0.8604}{\sqrt{R_{ex}}}. \tag{9.105}$$

Notice that at a fixed value of x this velocity does not diminish with vertical distance from the plate which may seem a little suprising given our notion that the region of flow disturbed by a body should be finite and the disturbance should die away. But remember that in the boundary layer approximation, the body is semi-infinite. In the real flow over a finite length plate where the boundary layer solution only applies over a limited region, the disturbance produced by the plate does die off at infinity.

The various thickness measures of the Blasius boundary layer are

$$\frac{\delta_{0.99}}{x} = \frac{4.906}{\sqrt{R_{ex}}} \qquad \frac{\delta^*}{x} = \frac{1.7208}{\sqrt{R_{ex}}} \qquad \frac{\theta}{x} = \frac{0.664}{\sqrt{R_{ex}}}. \tag{9.106}$$

In terms of the similarity variable, the edge of the boundary layer at $\delta_{0.99}$ is at $\alpha_e = 4.906/\sqrt{2} = 3.469$.

We can use (9.102) to get some insight into the legitimacy of the boundary layer idea whereby the flow is separated into a viscous region where the vorticity is non-zero and an inviscid region where the vorticity is zero as depicted in Figure 9.29.

The dimensionless vorticity (or shear stress) is given in (9.99). Let $\tau = F_{\alpha\alpha}$. The Blasius equation (9.102) can be espressed as follows.

$$\frac{d\tau}{\tau} = -F d\alpha \tag{9.107}$$

Integrate (9.107).

$$\frac{\tau}{\tau_w} = e^{-\int_0^\alpha F d\alpha} \tag{9.108}$$

The dimensionless stream function, the left panel in Figure 9.8, can be represented by

$$F(\alpha) = \alpha - G(\alpha). \tag{9.109}$$

The limiting behavior of G is $\lim_{\alpha \to \infty} G(\alpha) = C_1$ where C_1 is a positive constant related to the displacement thickness of the boundary layer. If we substitute (9.109) into (9.108) and integrate beyond the edge of the boundary layer the result is

$$\left.\frac{\tau}{\tau_w}\right|_{\alpha > \alpha_e} = e^{-\int_0^\alpha (\alpha - G(\alpha)) d\alpha} = C_2 e^{C_1 \alpha - \frac{\alpha^2}{2}}. \tag{9.110}$$

Equation (9.110) indicates that the shearing stress and vorticity decay exponentially at the edge of the layer. This rapid drop-off is a key point because it supports the fundamental idea of the boundary layer concept of separating the flow into two distinct zones.

9.7 THE FALKNER-SKAN BOUNDARY LAYERS

Finally, we address the question of free stream velocity distributions that lead to other similarity solutions beside the Blasius solution. We again analyze the stream function equation

$$\psi_y \psi_{xy} - \psi_x \psi_{yy} - U_e \frac{dU_e}{dx} - \nu \psi_{yyy} = 0. \tag{9.111}$$

Let

$$U_e = M x^\beta \tag{9.112}$$

where M has units

$$\hat{M} = L^{1-\beta}/T \ . \tag{9.113}$$

Similarity solutions of (9.111) exist for the class of power law freestream velocity distributions given by (9.112). This is the well-known Falkner-Skan family of boundary layers and the exponent β is the Falkner-Skan pressure gradient parameter.

The form of the similarity solution can be determined using a symmetry arguement similar to that used to solve the zero pressure gradient case. Insert (9.113) into (9.111). The governing equation becomes

$$\psi_y\psi_{xy} - \psi_x\psi_{yy} - \beta M^2 x^{(2\beta-1)} - \nu\psi_{yyy} = 0 \tag{9.114}$$

Now transform (9.114) using a three parameter dilation Lie group.

$$\tilde{x} = e^a x \qquad \tilde{y} = e^b y \qquad \tilde{\psi} = e^c \psi \tag{9.115}$$

Equation (9.114) transforms as

$$\begin{gathered}\tilde{\psi}_{\tilde{y}}\tilde{\psi}_{\tilde{x}\tilde{y}} - \tilde{\psi}_{\tilde{x}}\tilde{\psi}_{\tilde{y}\tilde{y}} - \beta M^2 \tilde{x}^{2\beta-1} - \nu\tilde{\psi}_{\tilde{y}\tilde{y}\tilde{y}} = \\ e^{2c-a-2b}(\psi_y\psi_{xy} - \psi_x\psi_{yy}) - e^{(2\beta-1)a}(\beta M^2 x^{2\beta-1}) - e^{c-3b}(\nu\tilde{\psi}_{\tilde{y}\tilde{y}\tilde{y}}) = 0\end{gathered} \ . \tag{9.116}$$

Equation (9.116) is invariant under the group (9.115) if and only if

$$2c - a - 2b = c - 3b = (2\beta - 1)a \ . \tag{9.117}$$

The boundaries of the problem at the wall and at infinity are invariant under (9.115).

$$\begin{gathered}\tilde{y} = e^b y = 0 \Rightarrow y = 0 \\ \tilde{\psi}(\tilde{x}, 0) = e^c \psi(e^a x, 0) = 0 \Rightarrow \psi(x, 0) = 0 \\ \tilde{\psi}_{\tilde{y}}(\tilde{x}, 0) = e^{c-b}\psi_y(e^a x, 0) = 0 \Rightarrow \psi_y(x, 0) = 0\end{gathered} \tag{9.118}$$

As in the case of the Blasius problem, the free stream boundary condition requires some care.

$$\tilde{\psi}_{\tilde{y}}(\tilde{x}, \infty) = e^{c-b}\psi_y(e^a x, \infty) = e^{\beta a} M x^{\beta} \tag{9.119}$$

The boundary condition at the outer edge of the boundary layer is invariant if and only if

$$c - b = \beta a \tag{9.120}$$

Solving (9.117) and (9.120) for a and c in terms of b leads to the group

$$\tilde{x} = e^{\frac{2}{1-\beta}b} x \qquad \tilde{y} = e^{b} y \qquad \tilde{\psi} = e^{\frac{1+\beta}{1-\beta}b} \psi \tag{9.121}$$

We can expect that the solution of the problem will be invariant under the group (9.121). That is we can expect a solution of the form

$$\frac{\psi}{x^{\left(\frac{1+\beta}{2}\right)}} = F\left(\frac{y}{x^{\left(\frac{1-\beta}{2}\right)}}\right) \tag{9.122}$$

As in the Blasius problem we use M and ν to nondimensionalize the problem. The similarity variables are,

$$\left.\begin{aligned} \alpha &= \left(\frac{M}{2\nu}\right)^{\frac{1}{2}} \frac{y}{(x+x_0)^{(1-\beta)/2}} \\ F &= \frac{\psi}{(x+x_0)^{(1+\beta)/2}(2\nu M)^{1/2}} \end{aligned}\right\}. \tag{9.123}$$

Upon substitution of (9.123) and (9.112), the streamfunction equation, (9.111) becomes,

$$\begin{aligned} &(x+x_0)^{2\beta-1}(F_\alpha((1+\beta)F-(1-\beta)\alpha F_\alpha)_\alpha - \\ &F_{\alpha\alpha}((1+\beta)F-(1-\beta)\alpha F_\alpha) - 2\beta - F_{\alpha\alpha\alpha}) = 0 \end{aligned} \tag{9.124}$$

Cancelling terms produces the Falkner-Skan equation,

$$F_{\alpha\alpha\alpha} + (1+\beta)FF_{\alpha\alpha} - 2\beta(F_\alpha)^2 + 2\beta = 0 \tag{9.125}$$

with boundary conditions,

$$F[0] = 0 \quad ; \qquad F_\alpha[0] = 0 \quad ; \qquad F_\alpha[\infty] = 1 \tag{9.126}$$

Note that $\beta = 0$ reduces (9.125) to the Blasius equation. It is fairly easy to reduce the order by one. The new variables are

$$\phi = F \quad ; \qquad G = F_\alpha \tag{9.127}$$

Differentiate

$$\frac{\frac{DG}{D\alpha}}{\frac{D\phi}{D\alpha}} = \frac{dG}{d\phi} = \frac{\frac{\partial G}{\partial \alpha}d\alpha + \frac{\partial G}{\partial F}dF + \frac{\partial G}{\partial F_\alpha}dF_\alpha}{\frac{\partial \beta}{\partial \alpha}d\alpha + \frac{\partial \beta}{\partial F}dF} = \frac{F_{\alpha\alpha}}{F_\alpha} \tag{9.128}$$

and

$$\frac{d^2G}{d\phi^2} = \left(\frac{F_\alpha F_{\alpha\alpha\alpha} - F_{\alpha\alpha}^2}{F_\alpha^2}\right)\frac{1}{F_\alpha} = \frac{F_\alpha(-(1+\beta)FF_{\alpha\alpha} + 2\beta(F_\alpha)^2 - 2\beta) - F_{\alpha\alpha}^2}{F_\alpha^3} \tag{9.129}$$

where the Falkner-Skan equation (9.125) has been used to replace the third derivative. Equation (9.129) can be rearranged to read

$$GG_{\phi\phi} + (1+\beta)\phi G_\phi + (G_\phi)^2 + 2\beta\left(\frac{1}{G} - G\right) = 0. \tag{9.130}$$

with the boundary conditions

$$G[0] = 0 \quad ; \qquad G[\infty] = 1 \ . \tag{9.131}$$

Several velocity profiles are shown in Figure 9.9.

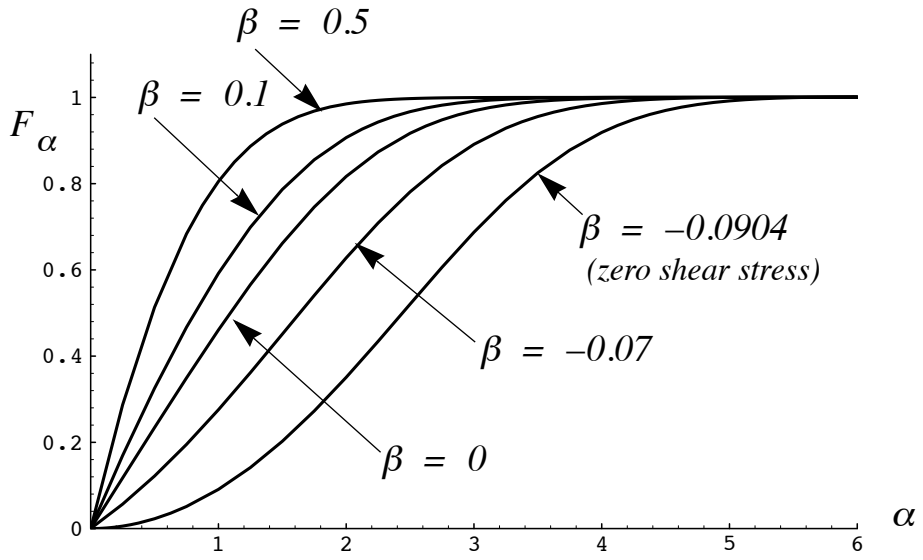

Figure 9.9 Falkner-Skan velocity profiles

The various measures of boundary layer thickness including shape factor (9.81), and wall stress are shown below.

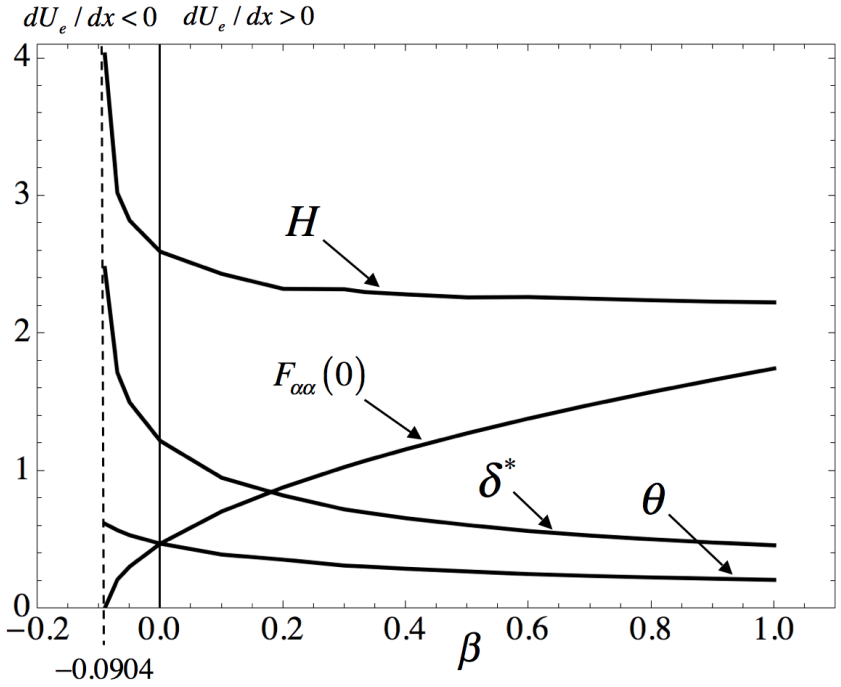

Figure 9.10 Falkner Skan boundary layer parameters versus β.

9.7.1 THE CASE $\beta = -1$

A particularly interesting case occurs when $\beta = -1$. The pressure gradient term is,

$$U_e = \frac{M}{x} \quad \Rightarrow \quad U_e \frac{dU_e}{dx} = -\frac{M^2}{x^3} \tag{9.132}$$

and the original variables become,

$$\left.\begin{aligned} \alpha &= \left(\frac{2\nu}{|M|}\right)\frac{y}{x + x_0} \\ F &= \pm\frac{\psi}{(2\nu|M|)^{1/2}} \end{aligned}\right\}. \tag{9.133}$$

The units of the governing parameter, $\hat{M} = L^2/T$, are the same as the kinematic viscosity and so the ratio $|M|/\nu$ is the (constant) Reynolds number for the $\beta = -1$ flow. The governing equation becomes

$$F_{\alpha\alpha\alpha} \pm (2(F_\alpha)^2 - 2) = 0 \tag{9.134}$$

The quantity M is an area flow rate and can change sign depending on whether the flow is created by a source or a sink. The plus sign corresponds to a source while the minus sign represents a sink. To avoid an imaginary root, the absolute value of M is used to nondimensionalize the stream function in (9.133). The once reduced equation is

$$G^2 G_{\phi\phi} + G G_\phi^{\,2} \pm 2(G^2 - 1) = 0 \tag{9.135}$$

where

$$\phi = F \quad ; \qquad G = F_\alpha . \tag{9.136}$$

Choose new variables

$$\gamma = G \quad ; \qquad H = G_\phi . \tag{9.137}$$

Differentiate the new variables in (9.137) with respect to ϕ and divide.

$$\frac{dH}{d\gamma} = \frac{H_\phi + H_G \dfrac{dG}{d\phi} + H_{G_\phi} \dfrac{dG_\phi}{d\phi}}{\gamma_\phi + \gamma_G \dfrac{dG}{d\phi}} = \frac{G_{\phi\phi}}{G_\phi} = \frac{-\dfrac{(G_\phi)^2}{G} - \dfrac{2}{G^2} + 2}{G_\phi} . \tag{9.138}$$

Equation (9.135) finally reduces to,

$$\frac{dH}{d\gamma} = \frac{-H^2\gamma \pm (2 - 2\gamma^2)}{\gamma^2 H} . \tag{9.139}$$

9.7.2 FALKNER-SKAN SINK FLOW

At this point we will restrict ourselves to the case of a sink flow (choose the minus sign in (9.135) and the plus sign in (9.139)). The flow we are considering is sketched below.

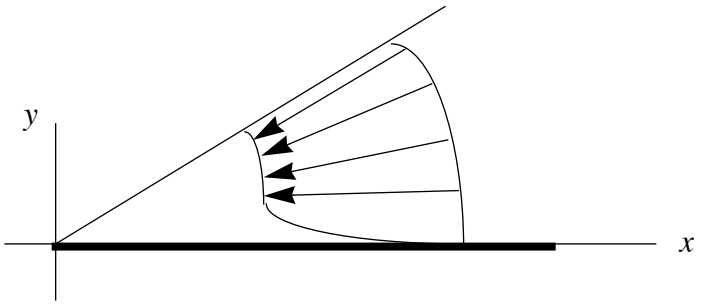

Figure 9.11 Falkner-Skan sink flow for $\beta = -1$.

The negative sign in front of the F in (9.133) insures that the velocity derived from the stream function is directed in the negative x direction. The first order ODE, (9.139) (with the minus sign selected) can be broken into the autonomous pair,

$$\left.\begin{aligned} \frac{dH}{ds} &= -H^2\gamma - 2 + 2\gamma^2 \\ \frac{d\gamma}{ds} &= \gamma^2 H \end{aligned}\right\} \tag{9.140}$$

with critical points at $(\gamma, H) = (0, \pm 1)$. The phase portrait of (9.140) is shown below.

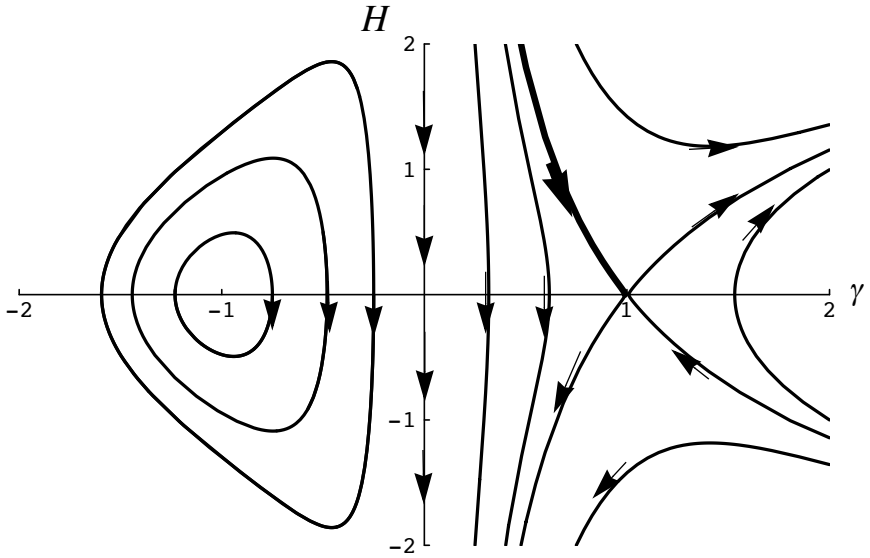

Figure 9.12 Phase portrait of the Falkner Skan case $\beta = -1$.

Equation (9.139) is rearranged to read,

$$(\gamma H^2 + 2 - 2\gamma^2)d\gamma + (\gamma^2 H)dH = 0 \tag{9.141}$$

which, by the cross derivative test can be shown to be a perfect differential with the integral,

$$C = 2\gamma - \frac{2}{3}\gamma^3 + \frac{1}{2}\gamma^2 H^2 . \tag{9.142}$$

Recall that,

$$\left.\begin{aligned} \gamma &= G = F_\alpha \\ H &= G_\phi = \frac{F_{\alpha\alpha}}{F_\alpha} \end{aligned}\right\}. \tag{9.143}$$

At the edge of the boundary layer,

$$\left.\begin{array}{l} \lim\limits_{\alpha \to \infty} F_\alpha = 1 \\ \lim\limits_{\alpha \to \infty} F_{\alpha\alpha} = 0 \end{array}\right\} \Rightarrow H[1] = 0 \ . \tag{9.144}$$

This allows us to evaluate C in (9.142). The result is,

$$C = \frac{4}{3} \ . \tag{9.145}$$

Solve (9.142) for H,

$$H = \left(\frac{4\gamma}{3} - \frac{4}{\gamma} + \frac{8}{3\gamma^2}\right)^{1/2} \quad ; \qquad (0 < \gamma < 1) \tag{9.146}$$

where the positive root is recognized to be the physical solution. The solution (9.146) is shown as the thicker weight trajectory in Figure 9.12. Equation (9.146) can be written as,

$$\gamma H = \sqrt{\frac{4}{3}}((\gamma - 1)^2(\gamma + 2))^{1/2} \tag{9.147}$$

In terms of the original variables

$$F_{\alpha\alpha} = \sqrt{\frac{4}{3}}((F_\alpha - 1)^2(F_\alpha + 2))^{1/2} \tag{9.148}$$

and

$$\alpha = Tanh^{-1}\left[\sqrt{\frac{F_\alpha + 2}{3}}\right] - Tanh^{-1}[\sqrt{2/3}] \tag{9.149}$$

The latter result can be solved for the negative of the velocity, F_α.

$$F_\alpha = 3Tanh^2[\alpha + Tanh^{-1}\sqrt{2/3}] - 2 \tag{9.150}$$

This is shown plotted below.

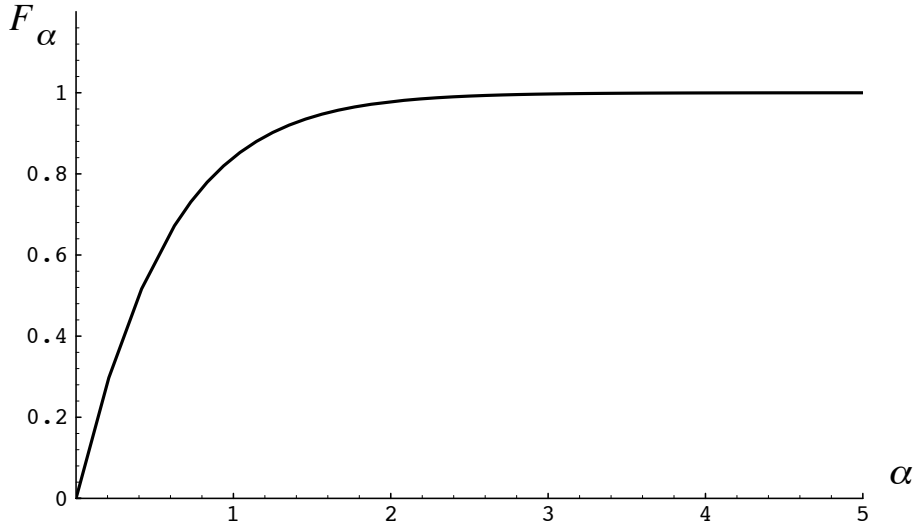

Figure 9.13 Falkner-Skan sink flow velocity profile $\beta = -1$.

The Falkner-Skan sink flow represents one of the few known exact solutions of the boundary layer equations. However the fact that an exact solution exists for the case $\beta = -1$ is no accident. Neither is the fact that this case corresponds to an independent variable of the form $\alpha \approx y/x$ where both coordinate directions are in some sense equivalent. Remember the essence of the boundary layer approximation was that the streamwise direction was in a sense "convective" while the transverse direction was regarded as "diffusive" producing a flow that is progressively more slender in the y direction as x increases. In the case of the Falkner-Skan sink flow the aspect ratio of the flow is constant.

9.8 THWAITES' METHOD FOR APPROXIMATE CALCULATION OF BOUNDARY LAYER CHARACTERISTICS

At the wall the momentum equation reduces to

$$\left.\frac{\partial^2 U}{\partial y^2}\right|_{y=0} = -\frac{U_e}{\nu}\frac{dU_e}{dx} \tag{9.151}$$

Rewrite (9.82) as

$$\left.\frac{\partial U}{\partial y}\right|_{y=0} = (2+H)\theta\frac{U_e}{\nu}\frac{dU_e}{dx} + \frac{U_e^2}{\nu}\frac{d\theta}{dx} \tag{9.152}$$

Choose θ and U_e as length and velocity scales to non-dimensionalize the left sides of (9.151) and (9.152).

$$\begin{aligned}\left(\frac{\theta^2}{U_e}\right)\left.\frac{\partial^2 U}{\partial y^2}\right|_{y=0} &= -\frac{\theta^2}{\nu}\frac{dU_e}{dx} \\ \left(\frac{\theta}{U_e}\right)\left.\frac{\partial U}{\partial y}\right|_{y=0} &= (2+H)\frac{\theta^2}{\nu}\frac{dU_e}{dx} + \frac{U_e}{2\nu}\frac{d\theta^2}{dx}\end{aligned} \tag{9.153}$$

In a landmark paper in 1948 Bryan Thwaites argued that the normalized derivatives on the left of (9.153) should depend only on the shape of the velocity profile and not explicitly on the free stream velocity or thickness. Morover he argued that there should be a universal function relating the two. He defined

$$m = \left(\frac{\theta^2}{U_e}\right)\left.\frac{\partial^2 U}{\partial y^2}\right|_{y=0} \qquad l(m) = \left(\frac{\theta}{U_e}\right)\left.\frac{\partial U}{\partial y}\right|_{y=0}. \tag{9.154}$$

In terms of m the Von Karman equation is

$$\frac{U_e}{\nu}\frac{d\theta^2}{dx} = 2((2+H)m + l(m)) = L(m) \tag{9.155}$$

where (9.151) has been used. Thwaites proceeded to examine a variety of known exact and approximate solutions of the boundary layer equations with a pressure gradient. The main results are shown below.

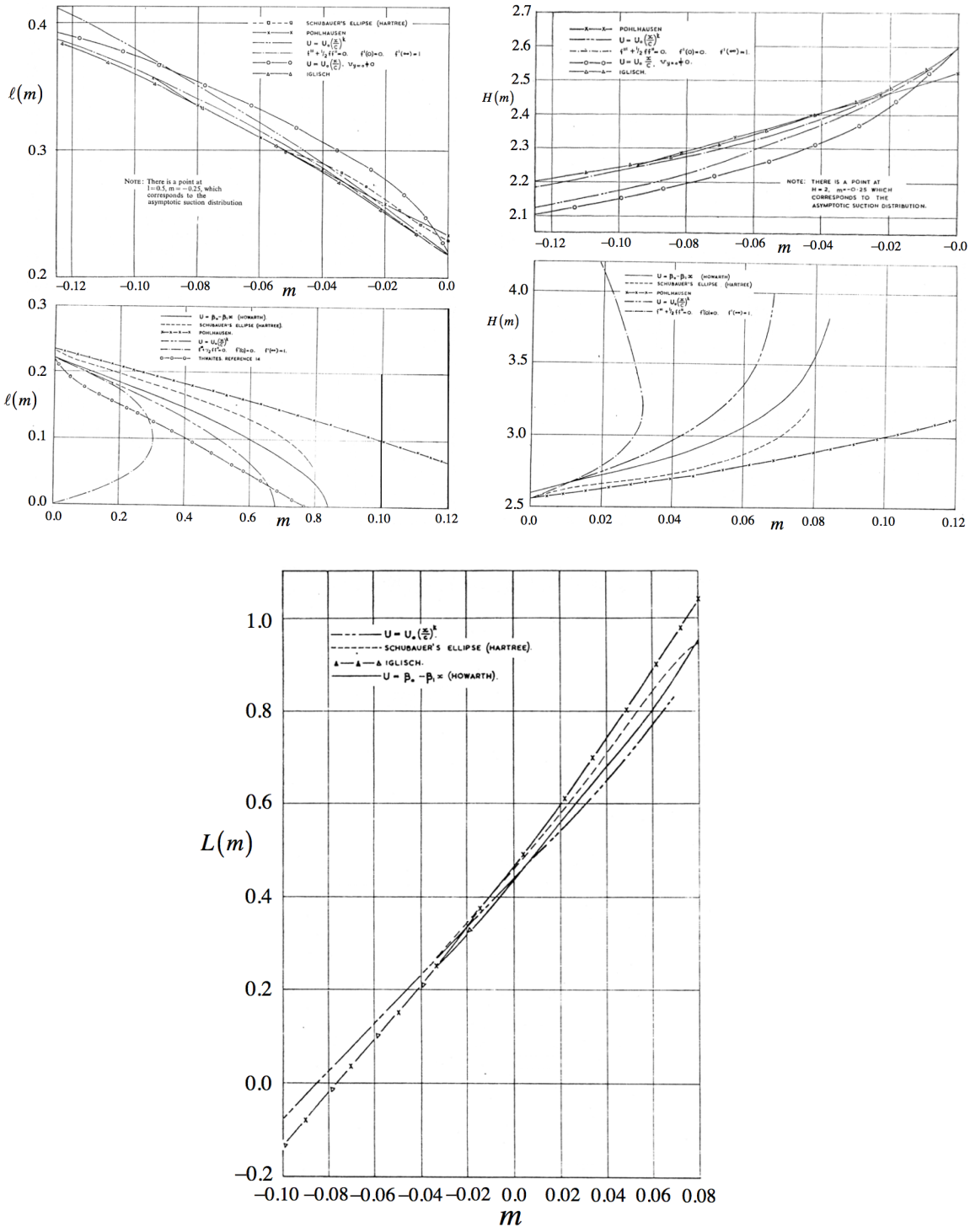

Figure 9.14 Data collected by Thwaites on skin friction, $l(m)$, shape factor $H(m)$ and $L(m)$ for a variety of boundary layer solutions.

The correlation of the data was remarkably good, especially the near straight line behavior of $L(m)$. Thwaites proposed the linear approximation

$$L(m) = 0.45 + 6m \tag{9.156}$$

One of the classes of solutions included in Thwaites' data is the Falkner-Skan boundary layers discussed earlier. For these solutions the Thwaites functions can be calculated explicitly.

$$\begin{aligned} m &= F_{\alpha\alpha\alpha}(0)\left(\int_0^\alpha F_\alpha(1-F_\alpha)d\alpha\right)^2 = -2\beta\left(\int_0^\alpha F_\alpha(1-F_\alpha)d\alpha\right)^2 \\ l(m) &= F_{\alpha\alpha}(0)\int_0^\alpha F_\alpha(1-F_\alpha)d\alpha \\ H(m) &= \frac{\int_0^\alpha (1-F_\alpha)d\alpha}{\int_0^\alpha F_\alpha(1-F_\alpha)d\alpha} \end{aligned} \tag{9.157}$$

The various measures of the Falkner-Skan solutions shown in Figure 9.10 can be related to m instead of β using the first equation in (9.157). The relation between m and β is shown below.

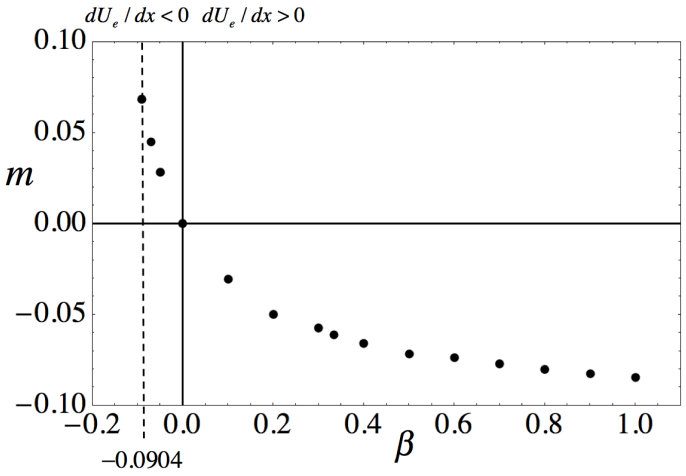

Figure 9.15 The variable m defined in (9.154) versus the free stream velocity exponent β for Falkner-Skan boundary layers.

The functions $l(m)$ and $H(m)$ for the Falkner-Skan boundary layer solutions are shown below.

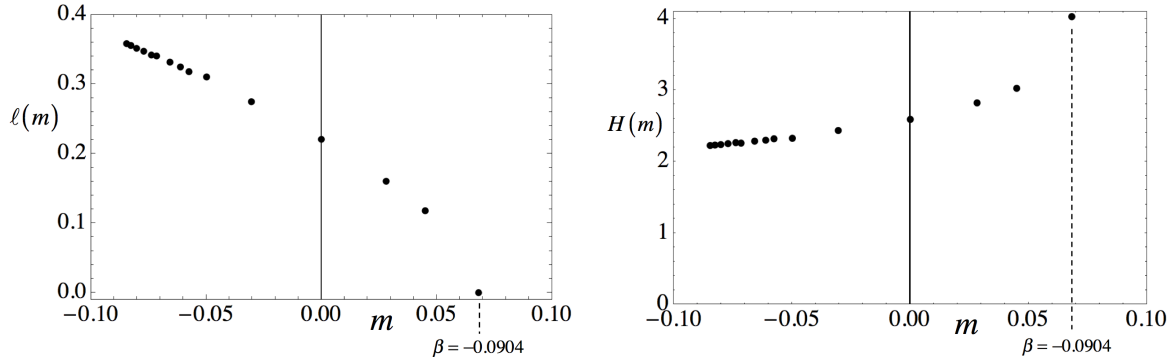

Figure 9.16 Thwaites functions for the Falkner-Skan solutions (9.157).

Thwaites' correlations were re-examined by N. Curle who came up with a very similar set of functions but with slightly improved prediction of boundary layer evolution in adverse pressure gradients. The figures below provide a comparison between the two methods.

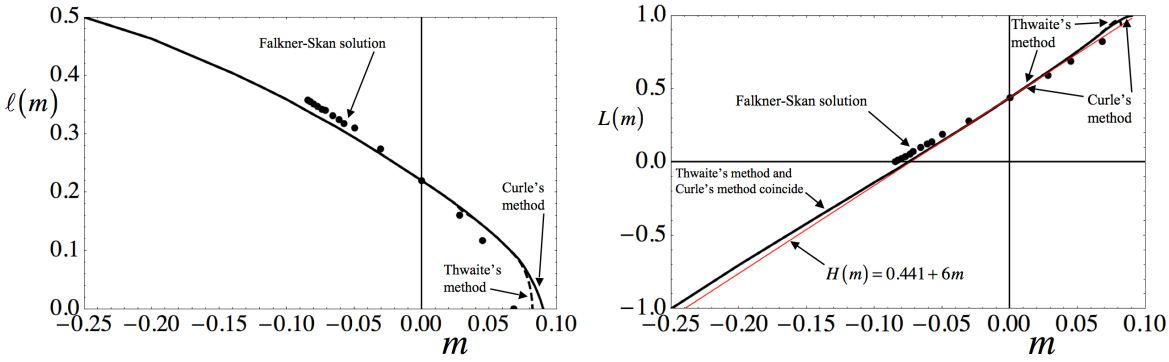

Figure 9.17 Comparison between Curle's functions and Thwaites' functions.

Curle's tabulation of his functions for Thwaites method is included below.

TABLE 5

Universal functions for Thwaites's method

m	$l(m)$	$H(m)$	m	$l(m)$	$H(m)$
−0·25	0·500	2·00	0·040	0·153	2·81
−0·20	0·463	2·07	0·048	0·138	2·87
−0·14	0·404	2·18	0·056	0·122	2·94
−0·12	0·382	2·23	0·060	0·113	2·99
−0·10	0·359	2·28	0·064	0·104	3·04
−0·080	0·333	2·34	0·068	0·095	3·09
−0·064	0·313	2·39	0·072	0·085	3·15
−0·048	0·291	2·44	0·076	0·072	3·22
−0·032	0·268	2·49	0·080	0·056	3·30
−0·016	0·244	2·55	0·084	0·038	3·39
0	0·220	2·61	0·086	0·027	3·44
+0·016	0·195	2·67	0·088	0·015	3·49
0·032	0·168	2·75	0·090	0	3·55

Figure 9.18 Curle's functions for Thwaites' method.

A reasonable linear approximation to the data for $L(m)$ in Figure 9.17 is

$$L(m) = 0.441 + 6m\,. \tag{9.158}$$

Equation (9.158) is not the best linear approximation to Curle's data in Figure 9.18 but is consistent with the value of the friction coefficient for the zero-pressure gradient Blasius boundary layer($\sqrt{0.441} = 0.664$). Insert (9.158) into (9.155) and use the definition of m in (9.153) and (9.154).

$$U_e \frac{d}{dx}\left(\frac{\theta^2}{\nu}\right) = 0.441 - 6\left(\frac{\theta^2}{\nu}\right)\frac{dU_e}{dx} \tag{9.159}$$

Equation (9.159) can be integrated exactly.

$$\theta^2 = \frac{0.441\nu}{U_e(x)^6}\int_0^x U_e(x')^5\,dx' \tag{9.160}$$

Equation (9.60) provides the momentum thickness of the boundary layer directly from the distribution of velocity outside the boundary layer $U_e(x)$. Although the von Karman integral equation (9.155) was used to generate the data for Thwaites' method, it is no longer needed once (9.160) is known.

The procedure for applying Thwaites' method is as follows.

1) Given $U_e(x)$, use (9.160) to determine $\theta^2(x)$.

At a given x:

2) The parameter m is determined from (9.154) and (9.151).

$$m = -\frac{\theta^2}{\nu}\frac{dU_e}{dx} \tag{9.161}$$

3) The functions $l(m)$ and $H(m)$ are determined from the data in Figure 9.18.

4)The friction coefficient is determined from

$$C_f = \frac{2\nu}{U_e\theta}l(m). \tag{9.162}$$

5) The displacement thickness $\delta^*(m)$ is determined from $H(m)$.

The process is repeated while progressing along the wall to increasing values of x. Separation of the boundary layer is assumed to have occurred if a point is reached where $l(m) = 0$.

The key references used in this section are

1) Thwaites, B. 1948 Approximate calculations of the laminar boundary layer, VII International Congress of Applied Mechanics, London. Also Aeronautical Quarterly Vol. 1, page 245, 1949.

2) Curle, N. 1962 The *Laminar Boundary Layer Equations*, Clarendon Press.

9.8.1 Example - Free stream velocity from potential flow over a circular cylinder.

To illustrate the application of Thwaites' method let's see what it predicts for the flow over a circular cylinder where we take as the free stream velocity the potential flow solution.

$$\frac{U_e}{U_\infty} = 2Sin\left(\frac{x}{R}\right) \tag{9.163}$$

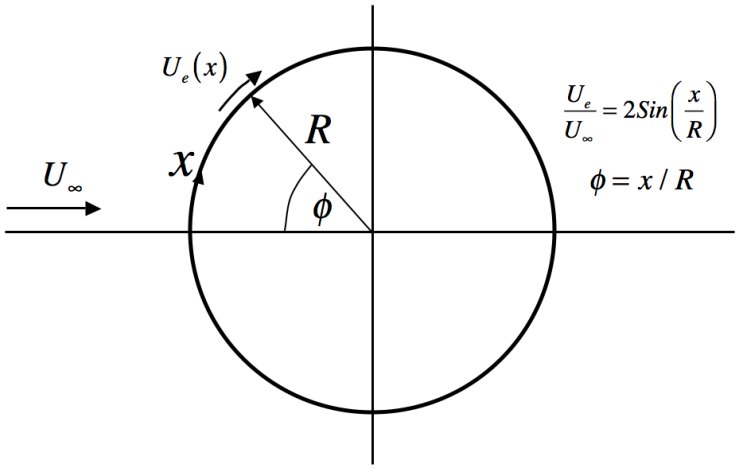

Figure 9.19 Example for Thwaites' method.

According to (9.160)

$$\left(\frac{\theta}{R}\right)^2 R_e = \frac{0.441}{Sin^6(\phi)} \int_0^\phi Sin^5(\phi')d\phi' \tag{9.164}$$

where

$$R_e = \frac{U_\infty 2R}{\nu} \tag{9.165}$$

Near the forward stagnation point

$$\lim_{\phi \to 0} \left(\frac{\theta}{R}\right)^2 R_e = \frac{0.441}{\phi^6} \int_0^\phi \phi^5 d\phi' = \frac{0.441}{6} \tag{9.166}$$

Interestingly the method gives a finite momentum thickness at the stagnation point. This is useful to know when we apply the method to an airfoil where the radius of the leading adge at the forward stagnation point will define the initial thickness for the boundary layer calculation. Next the relationship between m and ϕ is determined using (9.161).

$$m = -\frac{\theta^2}{\nu}\frac{dU_e}{dx} = -\frac{1}{2}\left(\frac{\theta}{R}\right)^2 R_e \frac{d}{d\phi}\left(\frac{U_e}{U_\infty}\right) = -\frac{0.441Cos(\phi)}{Sin^6(\phi)} \int_0^\phi Sin^5(\phi')d\phi' \tag{9.167}$$

Once $m(\phi)$ is known, $l(m(\phi))$ is determined from the data in Figure 9.18.

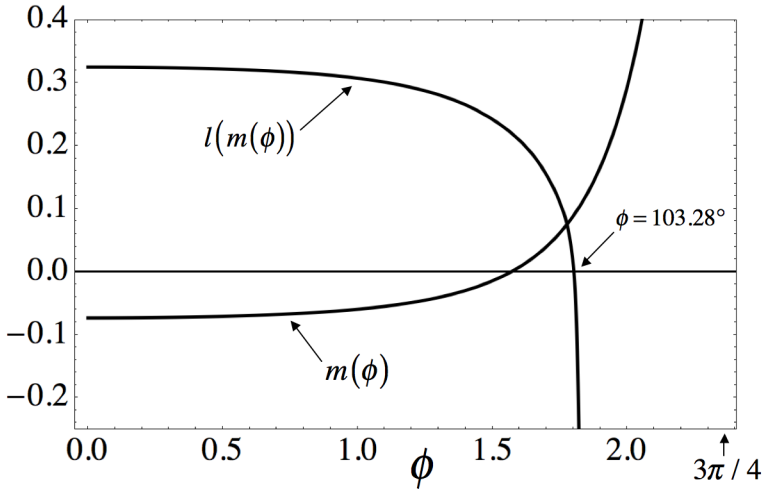

Figure 9.20 Thwaites' functions for the freestream distribution (9.163).

The friction coefficient determined using (9.162) is shown below.

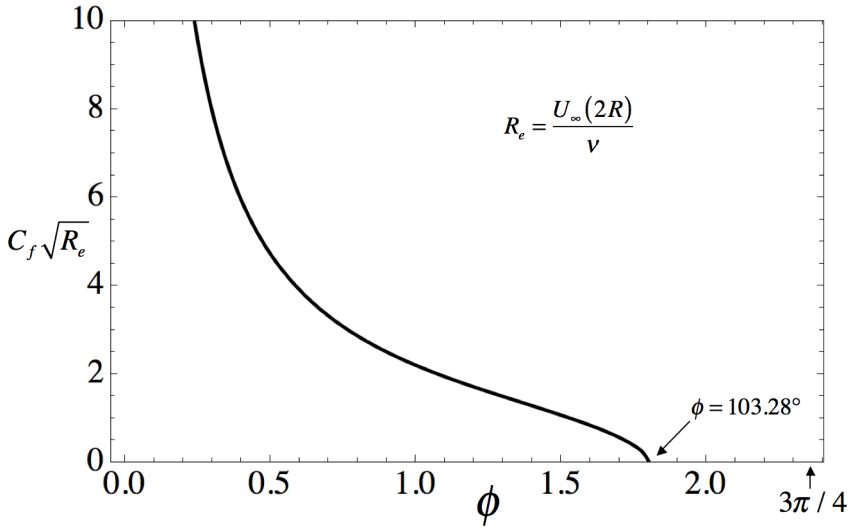

Figure 9.21 Friction coefficient for the freestream distribution (9.163).

According to this method the boundary layer on the cylinder would separate at $\phi = 103.28°$. The boundary layer parameters, momentum thickness, displacement thickness and shape factor, are shown below.

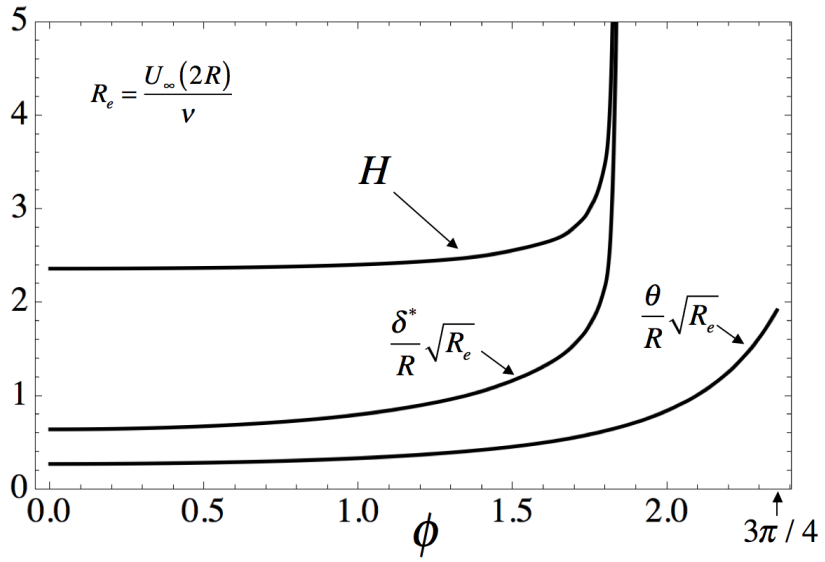

Figure 9.22 Boundary layer thicknesses and shape factor for the freestream distribution (9.163).

Notice the role of the Reynolds number. The momentum thickness and displacement thickness as well as the friction coefficient are all proportional to $1/\sqrt{R_e}$. We saw this same behavior in the Blasius solution, (9.104) and (9.106).

9.9 COMPRESSIBLE LAMINAR BOUNDARY LAYERS

The equations of motion for laminar flow are

$$\frac{\partial \rho U}{\partial x} + \frac{\partial \rho V}{\partial y} = 0$$

$$\rho U \frac{\partial U}{\partial x} + \rho V \frac{\partial U}{\partial y} = -\frac{dP_e}{dx} + \frac{\partial}{\partial y}\left(\mu \frac{\partial U}{\partial y}\right) \quad . \tag{9.168}$$

$$\rho U C_p \frac{\partial T}{\partial x} + \rho V C_p \frac{\partial T}{\partial y} = U \frac{dP_e}{dx} + \frac{\partial}{\partial y}\left(\kappa \frac{\partial T}{\partial y}\right) + \mu \left(\frac{\partial U}{\partial y}\right)^2$$

Using the same approach as in the Couette flow problem, let the temperature in the boundary layer layer be expressed as a function of the local velocity, $T = T(U)$. Substitute this functional form into the energy equation.

$$\left(\rho U\frac{\partial U}{\partial x}+\rho V\frac{\partial U}{\partial y}\right)C_p\frac{dT}{dU} \;=\; U\frac{dP}{dx}+\frac{\partial}{\partial y}\left(\kappa\frac{dT}{dU}\frac{\partial U}{\partial y}\right)+\mu\left(\frac{\partial U}{\partial y}\right)^2 \qquad (9.169)$$

Use the momentum equation to replace the factor in parentheses on the left hand side of (9.169).

$$\left(-\frac{dP}{dx}+\frac{\partial}{\partial y}\left(\mu\frac{\partial U}{\partial y}\right)\right)C_p\frac{dT}{dU} \;=\; U\frac{\partial P}{\partial x}+\frac{dT}{dU}\frac{\partial}{\partial y}\left(\kappa\frac{\partial U}{\partial y}\right)+\kappa\frac{d^2T}{dU^2}\left(\frac{\partial U}{\partial y}\right)^2+\mu\left(\frac{\partial U}{\partial y}\right)^2 \qquad (9.170)$$

which we can write as

$$-\frac{dP}{dx}\left(C_p\frac{dT}{dU}+U\right)+C_p\frac{dT}{dU}\frac{\partial}{\partial y}\left(\left(\mu-\frac{k}{C_p}\right)\frac{\partial U}{\partial y}\right)+\left(\kappa\frac{d^2T}{dU^2}+\mu\right)\left(\frac{\partial U}{\partial y}\right)^2 \;=\; 0\,. \qquad (9.171)$$

Introduce the Prandtl number (9.13) which can be assumed to be constant independent of position in the boundary layer. The energy equation becomes

$$-\frac{dP}{dx}\left(C_p\frac{dT}{dU}+U\right)+\frac{dT}{dU}\left(\frac{P_r-1}{P_r}\right)\frac{\partial}{\partial y}\left(\mu\frac{\partial U}{\partial y}\right)+\left(\kappa\frac{d^2T}{dU^2}+\mu\right)\left(\frac{\partial U}{\partial y}\right)^2 \;=\; 0\,. \qquad (9.172)$$

There are several important cases to consider.

9.9.1 Energy integral for a compressible boundary layer with an adiabatic wall and $P_r = 1$

In this case (9.172) reduces to

$$-\frac{dP}{dx}\left(C_p\frac{dT}{dU}+U\right)+\left(\kappa\frac{d^2T}{dU^2}+\mu\right)\left(\frac{\partial U}{\partial y}\right)^2 \;=\; 0\,. \qquad (9.173)$$

The flow at the wall satisfies

$$U\big|_{y=0} \;=\; 0 \qquad \left.\frac{dT}{dy}\right|_{y=0} \;=\; \left(\frac{dT}{dU}\frac{\partial U}{\partial y}\right)_{y=0} \;=\; 0\,. \qquad (9.174)$$

The velocity gradient at the wall is finite as is the wall shear stress $(\partial U/\partial y)_{y=0} \neq 0$ so the second condition in (9.174) implies that $(dT/dU)_{y=0} = 0$. The pressure gradient along the wall is not necessarily zero so flow conditions at the edge of the boundary layer can vary with the streamwise coordinate. The temperature must satisfy

$$\frac{d^2T}{dU^2} = -\frac{\mu}{\kappa} \tag{9.175}$$

and

$$\frac{dT}{dU} = -\frac{U}{C_p}. \tag{9.176}$$

Both (9.175) and (9.176) are consistent with the definition of the Prandtl number and the assumption $P_r = 1$ and integrate to

$$T_{wa} - T = \frac{1}{2C_p}U^2 \tag{9.177}$$

where T_{wa} is the adiabatic wall temperature defined in (9.20). This temperature can be expressed in terms of the temperature and velocity at the edge of the boundary layer.

$$T_{wa} = T_e + \frac{1}{2C_p}U_e^2 \tag{9.178}$$

Introduce the Mach number at the boundary layer edge $M_e = U_e/a_e$. Now

$$\frac{T_{wa}}{T_e} = 1 + \left(\frac{\gamma - 1}{2}\right)M_e^2 = \frac{T_{te}}{T_e}. \tag{9.179}$$

For a Prandtl number of one the stagnation temperature is constant through the boundary layer at the value at the boundary layer edge.

9.9.2 NON-ADIABATIC WALL WITH $dP/dx = 0$, AND $P_r = 1$

Again, although for different reasons than in the previous section, the temperature is governed by

$$\frac{d^2T}{dU^2} = -\frac{\mu}{\kappa}. \tag{9.180}$$

In this case, the temperature profile across the boundary layer is

$$C_p(T - T_w) + \frac{1}{2}U^2 = C_p\left(\frac{dT}{dU}\right)_{y=0} U. \tag{9.181}$$

where T_w is the temperature at the no-slip wall. The heat transfer rate at the wall is

$$Q_w = -\kappa\left(\frac{\partial T}{\partial y}\right)_{y=0} = -\kappa\left(\frac{dT}{dU}\frac{\partial U}{\partial y}\right)_{y=0} = -\frac{\kappa}{\mu}\left(\mu\frac{\partial U}{\partial y}\right)_{y=0}\left(\frac{dT}{dU}\right)_{y=0}. \tag{9.182}$$

Thus

$$C_p\left(\frac{dT}{dU}\right)_{y=0} = -\left(\frac{C_p\mu}{\kappa}\right)\frac{Q_w}{\tau_w}. \tag{9.183}$$

The temperature profile with heat transfer is

$$C_p(T - T_w) + \frac{1}{2}U^2 = -\frac{Q_w}{\tau_w}U \tag{9.184}$$

which is identical to the temperature profile (9.18) derived for the Couette flow case for $P_r = 1$. Evaluate (9.184) at the edge of the boundary layer where the velocity and temperature U_e and T_e are the same as the free stream values U_∞ and T_∞. The result is

$$T_w = T_\infty + \frac{1}{2C_p}U_\infty^{\,2} + \frac{Q_w}{\tau_w C_p}U_\infty. \tag{9.185}$$

The Stanton number was defined in the previous section on Couette flow

$$S_t = \frac{Q_w}{\rho_\infty U_\infty C_p (T_w - T_{wa})}. \tag{9.186}$$

The adiabatic wall temperature is the free stream stagnation temperature. Using (9.185) in (9.186) gives the friction coefficient in terms of the Stanton number.

$$C_f = 2S_t \tag{9.187}$$

which can be compared with the Couette flow result (9.29).

Using (9.184) and (9.185) the temperature profile can be expressed in terms of the free stream and wall temperatures as follows.

$$\frac{T - T_w}{T_\infty} = \left(1 - \frac{T_w}{T_\infty}\right)\frac{U}{U_\infty} + \left(\frac{U_\infty^2}{2C_p T_\infty}\right)\frac{U}{U_\infty}\left(1 - \frac{U}{U_\infty}\right) \tag{9.188}$$

9.10 Mapping a compressible to an incompressible boundary layer

In the late 1940's L. Howarth (Proc. R. Soc. London A 194, 16-42, 1948) and K. Stewartson (Proc. R. Soc. London A 200, 84-100, 1949) introduced a remarkable transformation that can be used to map the compressible boundary layer equations to the incompressible form including the effects of free stream velocity variation. The basic idea is to define a stream function for a virtual incompressible flow that carries the same mass flow, integrated to the wall, as the real compressible flow.

Figure 9.23 illustrates the idea. To satisfy the mass balance requirement, the constant density of the virtual flow is taken to be the stagnation density of the real flow at the edge of the boundary layer.

$$\rho_t = \rho_e\left(1 + \left(\frac{\gamma - 1}{2}\right)M_e^2\right)^{1/(\gamma - 1)} \tag{9.189}$$

The flow at the edge of the boundary layer is assumed to be isentropic

$$\frac{P_t}{P_e} = \left(\frac{T_t}{T_e}\right)^{\gamma/(\gamma - 1)} = \left(\frac{a_t}{a_e}\right)^{(2\gamma)/(\gamma - 1)} \tag{9.190}$$

The pressure through the boundary layer is constant, $P = P_e$ and $\tilde{P} = \tilde{P}_e$.

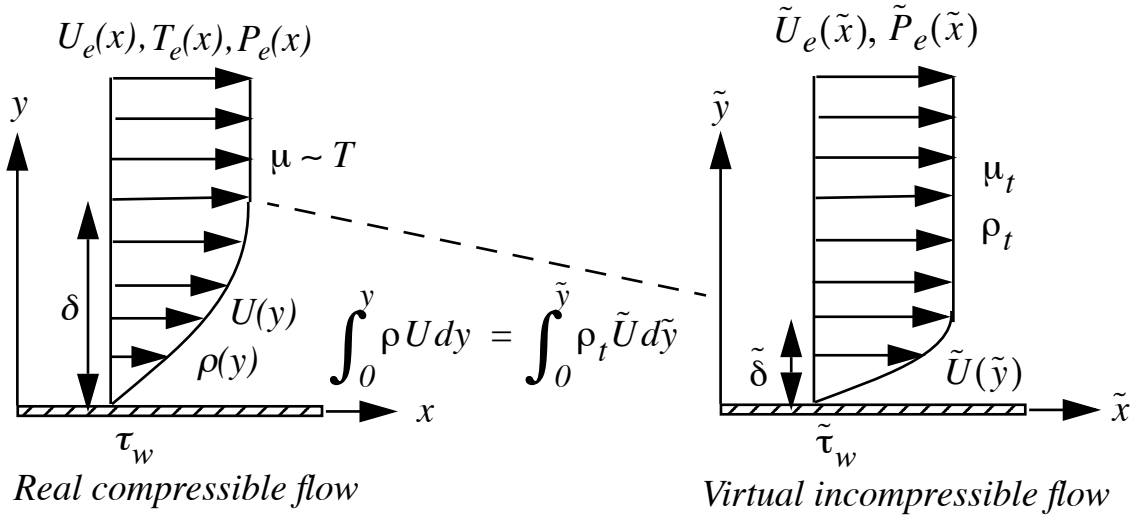

Figure 9.23 Mapping of a compressible flow to an incompressible flow.

Sutherland's law is referred to the stagnation temperature T_t of the compressible flow at the edge of the boundary layer.

$$\frac{\mu}{\mu_t} = \left(\frac{T}{T_t}\right)^{3/2}\left(\frac{T_t + T_S}{T + T_S}\right) \tag{9.191}$$

The viscosity of the virtual flow, μ_t, is the viscosity of the gas evaluated at T_t. The key assumption needed to make the mapping work is that the viscosity of the gas is linearly proportional to temperature.

$$\frac{\mu}{\mu_t} = \sigma\frac{T}{T_t} \tag{9.192}$$

where the constant σ is chosen to provide the best approximation of (9.191).

$$\sigma = \left(\frac{T_w}{T_t}\right)^{1/2}\left(\frac{T_t + T_S}{T_w + T_S}\right) \tag{9.193}$$

If $P_r = 1$ then $\sigma = 1$. The continuity and momentum equations governing the compressible flow are

$$\begin{aligned} \frac{\partial \rho U}{\partial x} + \frac{\partial \rho V}{\partial y} &= 0 \\ U\frac{\partial U}{\partial x} + V\frac{\partial U}{\partial y} &= -\frac{1}{\rho}\frac{dP_e}{dx} + \frac{1}{\rho}\frac{\partial}{\partial y}\left(\mu\frac{\partial U}{\partial y}\right) + \frac{1}{\rho}\frac{\partial \tau_{xy}}{\partial y} \end{aligned} \tag{9.194}$$

where it is understood that τ_{xy} refers to the turbulent shearing stress.

The coordinates of the virtual flow are defined as

$$\begin{aligned} \tilde{x} &= \sigma\int_0^x \left(\frac{P_e}{P_t}\left(\frac{a_e}{a_t}\right)\right) dx' = f(x) \\ \tilde{y} &= \left(\frac{a_e}{a_t}\right)\int_0^y \left(\frac{\rho(x, y')}{\rho_t}\right) dy' = g(x, y) \end{aligned} \tag{9.195}$$

Note that $\tilde{y}$ is a function of x and y since the density depends on both spatial variables. The variables x' and y' are dummy variables of integration. From the fundamental theorem of calculus the derivatives of the coodinates are

$$\begin{aligned} \frac{\partial \tilde{x}}{\partial x} &= f_x = \sigma\left(\frac{P_e}{P_t}\left(\frac{a_e}{a_t}\right)\right) \\ \frac{\partial \tilde{x}}{\partial y} &= f_y = 0 \\ \frac{\partial \tilde{y}}{\partial x} &= g_x \\ \frac{\partial \tilde{y}}{\partial y} &= g_y = \left(\frac{a_e}{a_t}\right)\left(\frac{\rho}{\rho_t}\right) \end{aligned} \tag{9.196}$$

Each of the derivatives is known explicitly except $\partial\tilde{y}/\partial x$. However, as we will see in the analysis to follow, terms that involve this derivative will cancel.

The continuity equation is satisfied identically through the introduction of a compressible stream function. Let

$$\rho U = \rho_t \frac{\partial \psi}{\partial y} \qquad \rho V = -\rho_t \frac{\partial \psi}{\partial x} \tag{9.197}$$

The stream function of the virtual incompressible flow is a function of $\tilde{x}(x)$ and $\tilde{y}(x, y)$ and has the same value as its counterpart in the real compressible flow since there is the same mass flow between the streamline and the wall in the two flows.

$$\psi(x, y) = \tilde{\psi}(\tilde{x}(x), \tilde{y}(x, y)) \tag{9.198}$$

The mapping we are about to carry out is a bit complicated. In the discussion below I have tried to retain as much detail as possible to help the reader get through the derivation without requiring a lot of side work to see how one relation follows from another. Maybe there is more detail than needed but I decided to err on the side of more rather than less to try to give maximum help to the reader.

According to the chain the partial derivatives of ψ in (9.197) are

$$\begin{aligned} \frac{\partial \psi}{\partial x} &= \frac{\partial \tilde{\psi}}{\partial \tilde{x}}\frac{\partial \tilde{x}}{\partial x} + \frac{\partial \tilde{\psi}}{\partial \tilde{y}}\frac{\partial \tilde{y}}{\partial x} = \frac{\partial \tilde{\psi}}{\partial \tilde{x}}\frac{d\tilde{x}}{dx} + \frac{\partial \tilde{\psi}}{\partial \tilde{y}}\frac{\partial \tilde{y}}{\partial x} \\ \frac{\partial \psi}{\partial y} &= \frac{\partial \tilde{\psi}}{\partial \tilde{x}}\frac{\partial \tilde{x}}{\partial y} + \frac{\partial \tilde{\psi}}{\partial \tilde{y}}\frac{\partial \tilde{y}}{\partial y} = \frac{\partial \tilde{\psi}}{\partial \tilde{y}}\frac{\partial \tilde{y}}{\partial y} \end{aligned} \tag{9.199}$$

The velocities can be expressed in terms of the new coodinates as.

$$\begin{aligned} U &= \frac{\rho_t}{\rho}\frac{\partial \psi}{\partial y} = \left(\frac{a_e}{a_t}\right)\frac{\partial \tilde{\psi}}{\partial \tilde{y}} = \left(\frac{a_e}{a_t}\right)\tilde{U} \\ V &= -\frac{\rho_t}{\rho}\frac{\partial \psi}{\partial x} = -\sigma\frac{\rho_t}{\rho}\left(\frac{P_e}{P_t}\frac{a_e}{a_t}\right)\frac{\partial \tilde{\psi}}{\partial \tilde{x}} - \frac{\rho_t}{\rho}\frac{\partial \tilde{\psi}}{\partial \tilde{y}}\frac{\partial \tilde{y}}{\partial x} \end{aligned} \tag{9.200}$$

The streamwise velocity in the virtual flow is $\tilde{U} = \partial\tilde{\psi}/\partial\tilde{y}$. The mass flow between the streamline and the wall in the two flows is depicted in Figure 9.23.

$$\int_0^y \rho U dy = \int_0^{\tilde{y}} \rho_t \tilde{U} d\tilde{y} \tag{9.201}$$

Differentiate (9.201) at a fixed x and use (9.200). The result is

$$\frac{d\tilde{y}}{dy} = \frac{\rho U}{\rho_t \tilde{U}} = \left(\frac{a_e}{a_t}\right)\frac{\rho}{\rho_t} \tag{9.202}$$

which is consistent with the partial derivative $\partial\tilde{y}/\partial y$ in (9.196). Equation (9.202) confirms that the definition of $\tilde{y}$ defined in (9.195) insures that the streamline values in the two flows are the same, that (9.198) holds.

Use the chain rule to determine the first derivatives of U that appear in (9.194).

$$\frac{\partial U}{\partial x} = \frac{\partial}{\partial\tilde{x}}\left(\left(\frac{a_e}{a_t}\right)\frac{\partial\tilde{\psi}}{\partial\tilde{y}}\right)\frac{d\tilde{x}}{dx} + \frac{\partial}{\partial\tilde{y}}\left(\left(\frac{a_e}{a_t}\right)\frac{\partial\tilde{\psi}}{\partial\tilde{y}}\right)\frac{\partial\tilde{y}}{\partial x} =$$

$$\sigma\left(\frac{P_e}{P_t}\left(\frac{a_e}{a_t}\right)^2\right)\left(\left(\frac{1}{a_e}\right)\frac{\partial a_e}{\partial\tilde{x}}\frac{\partial\tilde{\psi}}{\partial\tilde{y}} + \frac{\partial^2\tilde{\psi}}{\partial\tilde{x}\partial\tilde{y}}\right) + \left(\frac{a_e}{a_t}\right)\frac{\partial^2\tilde{\psi}}{\partial\tilde{y}^2}\frac{\partial\tilde{y}}{\partial x} \tag{9.203}$$

$$\frac{\partial U}{\partial y} = \frac{\partial}{\partial\tilde{x}}\left(\left(\frac{a_e}{a_t}\right)\frac{\partial\tilde{\psi}}{\partial\tilde{y}}\right)\frac{\partial\tilde{x}}{\partial y} + \frac{\partial}{\partial\tilde{y}}\left(\left(\frac{a_e}{a_t}\right)\frac{\partial\tilde{\psi}}{\partial\tilde{y}}\right)\frac{\partial\tilde{y}}{\partial y} = \left(\frac{a_e}{a_t}\right)^2\left(\frac{\rho}{\rho_t}\right)\left(\frac{\partial^2\tilde{\psi}}{\partial\tilde{y}^2}\right)$$

Now we can form the convective terms in (9.194).

$$U\frac{\partial U}{\partial x} + V\frac{\partial U}{\partial y} =$$

$$\sigma\left(\frac{P_e}{P_t}\left(\frac{a_e}{a_t}\right)^3\right)\left(\left(\frac{1}{a_e}\right)\frac{\partial a_e}{\partial\tilde{x}}\left(\frac{\partial\tilde{\psi}}{\partial\tilde{y}}\right)^2 + \frac{\partial\tilde{\psi}}{\partial\tilde{y}}\frac{\partial^2\tilde{\psi}}{\partial\tilde{x}\partial\tilde{y}}\right) + \left(\frac{a_e}{a_t}\right)^2\frac{\partial\tilde{\psi}}{\partial\tilde{y}}\left(\frac{\partial^2\tilde{\psi}}{\partial\tilde{y}^2}\frac{\partial\tilde{y}}{\partial x}\right) - \tag{9.204}$$

$$\left((\sigma)\left(\frac{P_e}{P_t}\frac{a_e}{a_t}\right)\left(\frac{a_e}{a_t}\right)^2\left(\frac{\partial^2\tilde{\psi}}{\partial\tilde{y}^2}\right)\frac{\partial\tilde{\psi}}{\partial\tilde{x}} + \left(\frac{a_e}{a_t}\right)^2\left(\frac{\partial^2\tilde{\psi}}{\partial\tilde{y}^2}\right)\frac{\partial\tilde{\psi}}{\partial\tilde{y}}\frac{\partial\tilde{y}}{\partial x}\right)$$

Note the terms involving $\partial\tilde{y}/\partial x$ cancel in (9.204). Thus

$$U\frac{\partial U}{\partial x} + V\frac{\partial U}{\partial y} =$$
$$\sigma\left(\frac{P_e}{P_t}\left(\frac{a_e}{a_t}\right)^3\right)\left(\left(\frac{1}{a_e}\right)\frac{\partial a_e}{\partial \tilde{x}}\left(\frac{\partial \tilde{\psi}}{\partial \tilde{y}}\right)^2 + \frac{\partial \tilde{\psi}}{\partial \tilde{y}}\frac{\partial^2 \tilde{\psi}}{\partial \tilde{x}\,\partial \tilde{y}} - \left(\frac{\partial^2 \tilde{\psi}}{\partial \tilde{y}^2}\right)\frac{\partial \tilde{\psi}}{\partial \tilde{x}}\right) \tag{9.205}$$

Now consider the pressure gradient term. Assume the flow at the edge of the boundary layer is isentropic.

$$\left(\frac{P_e}{P_t}\right) = \left(\frac{a_e}{a_t}\right)^{\frac{2\gamma}{(\gamma-1)}} \tag{9.206}$$

The pressure gradient term can be expressed in terms of the speed of sound at the boundary layer edge.

$$\frac{dP_e}{dx} = \frac{2\gamma P_t}{(\gamma-1)}\left(\frac{a_e}{a_t}\right)^{\frac{\gamma+1}{\gamma-1}}\frac{1}{a_t}\frac{da_e}{d\tilde{x}}\frac{d\tilde{x}}{dx} = \sigma\left(\frac{P_e}{P_t}\left(\frac{a_e}{a_t}\right)\right)\frac{2\gamma P_t}{(\gamma-1)}\left(\frac{a_e}{a_t}\right)^{\frac{\gamma+1}{\gamma-1}}\frac{1}{a_t}\frac{da_e}{d\tilde{x}} \tag{9.207}$$
$$\frac{dP_e}{dx} = \sigma\left(\frac{P_e}{P_t}\left(\frac{a_e}{a_t}\right)^2\right)\left(\frac{2\gamma P_t}{(\gamma-1)}\left(\frac{a_e}{a_t}\right)^{\frac{\gamma+1}{\gamma-1}}\frac{1}{a_e}\frac{da_e}{d\tilde{x}}\right)$$

Now

$$U\frac{\partial U}{\partial x} + V\frac{\partial U}{\partial y} + \frac{1}{\rho}\frac{dP_e}{dx} =$$
$$\sigma\left(\frac{P_e}{P_t}\left(\frac{a_e}{a_t}\right)^3\right)\left(\frac{\partial \tilde{\psi}}{\partial \tilde{y}}\frac{\partial^2 \tilde{\psi}}{\partial \tilde{x}\,\partial \tilde{y}} - \left(\frac{\partial^2 \tilde{\psi}}{\partial \tilde{y}^2}\right)\frac{\partial \tilde{\psi}}{\partial \tilde{x}}\right) + \tag{9.208}$$
$$\sigma\left(\frac{P_e}{P_t}\left(\frac{a_e}{a_t}\right)^3\right)\left(\left(\frac{\partial \tilde{\psi}}{\partial \tilde{y}}\right)^2 + \frac{1}{\rho}\frac{2\gamma P_t}{(\gamma-1)}\left(\frac{a_e}{a_t}\right)^{\frac{2}{\gamma-1}}\right)\left(\left(\frac{1}{a_e}\right)\frac{da_e}{d\tilde{x}}\right)$$

Note that, from (9.200)

$$\left(\frac{\partial\tilde{\psi}}{\partial\tilde{y}}\right)^2 = U^2\left(\frac{a_t}{a_e}\right)^2 . \tag{9.209}$$

So far

$$\begin{aligned} U\frac{\partial U}{\partial x} + V\frac{\partial U}{\partial y} + \frac{1}{\rho}\frac{dP_e}{dx} = \\ \sigma\left(\frac{P_e}{P_t}\left(\frac{a_e}{a_t}\right)^3\right)\left(\frac{\partial\tilde{\psi}}{\partial\tilde{y}}\frac{\partial^2\tilde{\psi}}{\partial\tilde{x}\partial\tilde{y}} - \left(\frac{\partial^2\tilde{\psi}}{\partial\tilde{y}^2}\right)\frac{\partial\tilde{\psi}}{\partial\tilde{x}}\right) + \\ \sigma\left(\frac{P_e}{P_t}\left(\frac{a_e}{a_t}\right)^3\right)\left(U^2\left(\frac{a_t}{a_e}\right)^2 + \frac{1}{\rho}\frac{2\gamma P_t}{(\gamma-1)}\left(\frac{a_e}{a_t}\right)^{\frac{2}{\gamma-1}}\right)\left(\left(\frac{1}{a_e}\right)\frac{da_e}{d\tilde{x}}\right) \end{aligned} . \tag{9.210}$$

The flow at the edge of the boundary layer is adiabatic.

$$a_t^2 = a_e^2 + \left(\frac{\gamma-1}{2}\right)U_e^2 \tag{9.211}$$

and

$$\frac{1}{a_e}\frac{da_e}{d\tilde{x}} = -\left(\frac{\gamma-1}{2a_e^2}\right)U_e\frac{dU_e}{d\tilde{x}} \tag{9.212}$$

Now

$$\begin{aligned} U\frac{\partial U}{\partial x} + V\frac{\partial U}{\partial y} + \frac{1}{\rho}\frac{dP_e}{dx} = \\ \sigma\left(\frac{P_e}{P_t}\left(\frac{a_e}{a_t}\right)^3\right)\left(\frac{\partial\tilde{\psi}}{\partial\tilde{y}}\frac{\partial^2\tilde{\psi}}{\partial\tilde{x}\partial\tilde{y}} - \left(\frac{\partial^2\tilde{\psi}}{\partial\tilde{y}^2}\right)\frac{\partial\tilde{\psi}}{\partial\tilde{x}}\right) - \\ \sigma\left(\frac{P_e}{P_t}\left(\frac{a_e}{a_t}\right)^3\right)\left(U^2\frac{(\gamma-1)}{2a_e^2}\left(\frac{a_t}{a_e}\right)^2 + \frac{1}{\rho}\frac{\gamma P_t}{a_e^2}\left(\frac{a_e}{a_t}\right)^{\frac{2}{\gamma-1}}\right)\left(U_e\frac{dU_e}{d\tilde{x}}\right) \end{aligned} . \tag{9.213}$$

Note that

$$U^2\frac{(\gamma-1)}{2a_e^2}\left(\frac{a_t}{a_e}\right)^2+\frac{1}{\rho}\frac{\gamma P_t}{a_e^2}\left(\frac{a_e}{a_t}\right)^{\frac{2}{\gamma-1}}=$$

$$U^2\frac{(\gamma-1)}{2a_e^2}\left(\frac{a_t}{a_e}\right)^2+\frac{\rho_e}{\rho}\frac{\gamma P_e}{\rho_e}\frac{1}{a_e^2}\left(\frac{a_t}{a_e}\right)^{\frac{2\gamma}{\gamma-1}}\left(\frac{a_e}{a_t}\right)^{\frac{2}{\gamma-1}}= \tag{9.214}$$

$$\left(\frac{a_t}{a_e}\right)^4\left(\frac{a^2+\frac{(\gamma-1)}{2}U^2}{a_t^2}\right)$$

where we have used the isentropic relation $P_t/P_e=(a_t/a_e)^{2\gamma/(\gamma-1)}$ and $\gamma P_e/\rho=(\gamma P)/\rho=a^2$. Now work out the viscous term using $\rho T=P/R=P_e/R$.

$$\tau_{xy}|_{laminar}=\mu\frac{\partial U}{\partial y}=\sigma\mu_t\left(\frac{T}{T_t}\right)\frac{\partial}{\partial y}\left(\left(\frac{a_e}{a_t}\right)\frac{\partial\tilde{\psi}}{\partial\tilde{y}}\right)=\sigma\mu_t\left(\frac{T}{T_t}\right)\left(\frac{a_e}{a_t}\right)\frac{\partial}{\partial y}\left(\frac{\partial\tilde{\psi}}{\partial\tilde{y}}\right)=$$

$$\sigma\mu_t\left(\frac{a_e}{a_t}\right)^2\left(\frac{T}{T_t}\right)\left(\frac{\rho}{\rho_t}\right)\frac{\partial}{\partial\tilde{y}}\left(\frac{\partial\tilde{\psi}}{\partial\tilde{y}}\right)=\sigma\left(\frac{a_e}{a_t}\right)^2\left(\frac{\rho T}{\rho_t T_t}\right)\left(\mu_t\frac{\partial\tilde{U}}{\partial\tilde{y}}\right)=\sigma\left(\frac{a_e}{a_t}\right)^2\left(\frac{P_e}{P_t}\right)\tilde{\tau}_{\tilde{x}\tilde{y}}|_{laminar} \tag{9.215}$$

Recall $\tilde{U}=\partial\tilde{\psi}/\partial\tilde{y}$ and $\tilde{\tau}_{\tilde{x}\tilde{y}}|_{laminar}=\mu_t\partial\tilde{U}/\partial\tilde{y}$. The viscous stress term in the boundary layer equation is

$$\frac{1}{\rho}\frac{\partial}{\partial y}\left(\mu\frac{\partial U}{\partial y}\right)=\sigma\frac{\mu_t}{\rho_t}\frac{P_e}{P_t}\left(\frac{a_e}{a_t}\right)^3\left(\frac{\partial^3\tilde{\psi}}{\partial\tilde{y}^3}\right). \tag{9.216}$$

The turbulent stress term transforms as

$$\tilde{\tau}_{xy}\Big|_{turbulent}=\frac{1}{\sigma}\left(\left(\frac{a_t}{a_e}\right)^2\frac{P_t}{P_e}\right)\tau_{xy}\Big|_{turbulent}. \tag{9.217}$$

which can be expressed as

$$\frac{1}{\rho}\frac{\partial}{\partial y}\left(\tau_{xy}\Big|_{turbulent}\right) = \sigma\frac{1}{\rho_t}\frac{P_e}{P_t}\left(\frac{a_e}{a_t}\right)^3\frac{\partial}{\partial\tilde{y}}\left(\tilde{\tau}_{xy}\Big|_{turbulent}\right). \tag{9.218}$$

Now the boundary layer momentum equation (9.194)becomes

$$\begin{aligned} U\frac{\partial U}{\partial x} + V\frac{\partial U}{\partial y} + \frac{1}{\rho}\frac{dP_e}{dx} - \frac{1}{\rho}\frac{\partial}{\partial y}\left(\mu\frac{\partial U}{\partial y}\right) - \frac{1}{\rho}\frac{\partial\tau_{xy}}{\partial y} = \\ \sigma\left(\frac{P_e}{P_t}\left(\frac{a_e}{a_t}\right)^3\right)\left(\frac{\partial\tilde{\psi}}{\partial\tilde{y}}\frac{\partial^2\tilde{\psi}}{\partial\tilde{x}\partial\tilde{y}} - \left(\frac{\partial^2\tilde{\psi}}{\partial\tilde{y}^2}\right)\frac{\partial\tilde{\psi}}{\partial\tilde{x}}\right) - \\ \sigma\left(\frac{P_e}{P_t}\left(\frac{a_e}{a_t}\right)^3\right)\left(\left(\frac{a_t}{a_e}\right)^4\left(\frac{a^2 + \frac{(\gamma-1)}{2}U^2}{a_t^2}\right)\right)\left(U_e\frac{dU_e}{d\tilde{x}}\right) - \\ \sigma\frac{\mu_t}{\rho_t}\frac{P_e}{P_t}\left(\frac{a_e}{a_t}\right)^3\left(\frac{\partial^3\tilde{\psi}}{\partial\tilde{y}^3}\right) - \sigma\frac{1}{\rho_t}\frac{P_e}{P_t}\left(\frac{a_e}{a_t}\right)^3\frac{\partial}{\partial\tilde{y}}\left(\tilde{\tau}_{xy}\Big|_{turbulent}\right) = 0 \end{aligned} \tag{9.219}$$

Drop the common factor multiplying each term on the right of (9.219). The transformed equation is nearly in incompressible form.

$$\begin{aligned} \left(\frac{\partial\tilde{\psi}}{\partial\tilde{y}}\frac{\partial^2\tilde{\psi}}{\partial\tilde{x}\partial\tilde{y}} - \left(\frac{\partial^2\tilde{\psi}}{\partial\tilde{y}^2}\right)\frac{\partial\tilde{\psi}}{\partial\tilde{x}}\right) - \left(\frac{a_t}{a_e}\right)^4\left(\frac{a^2 + \frac{(\gamma-1)}{2}U^2}{a_t^2}\right)U_e\frac{dU_e}{d\tilde{x}} - \\ \frac{\mu_t}{\rho_t}\left(\frac{\partial^3\tilde{\psi}}{\partial\tilde{y}^3}\right) - \frac{1}{\rho_t}\frac{\partial}{\partial\tilde{y}}(\tilde{\tau}_{xy}\Big|_{turbulent}) = 0 \end{aligned} \tag{9.220}$$

The real and virtual free stream velocities are related by

$$\tilde{U}_e = \frac{a_t}{a_e}U_e. \tag{9.221}$$

which comes from the expression for U in (9.200). Differentiate (9.221)

$$\tilde{U}_e \frac{d\tilde{U}_e}{d\tilde{x}} = \left(\frac{a_t}{a_e}\right)^2 \left(\frac{1}{a_e^2}\right)\left(a_e^2 + \left(\frac{\gamma-1}{2}\right)U_e^2\right) U_e \frac{dU_e}{d\tilde{x}} = \left(\frac{a_t}{a_e}\right)^4 U_e \frac{dU_e}{d\tilde{x}} \tag{9.222}$$

and substitute (9.222) into (9.220).

$$\left(\frac{\partial\tilde{\psi}}{\partial\tilde{y}}\frac{\partial^2\tilde{\psi}}{\partial\tilde{x}\partial\tilde{y}} - \left(\frac{\partial^2\tilde{\psi}}{\partial\tilde{y}^2}\right)\frac{\partial\tilde{\psi}}{\partial\tilde{x}}\right) - \left(\frac{a^2 + \frac{(\gamma-1)}{2}U^2}{a_t^2}\right)\tilde{U}_e\frac{d\tilde{U}_e}{d\tilde{x}} - \frac{\mu_t}{\rho_t}\left(\frac{\partial^3\tilde{\psi}}{\partial\tilde{y}^3}\right) - \frac{1}{\rho_t}\frac{\partial}{\partial\tilde{y}}\left(\tilde{\tau}_{xy}\Big|_{turbulent}\right) = 0 \tag{9.223}$$

The velocities in the virtual flow are

$$\tilde{U} = \frac{\partial\tilde{\psi}}{\partial\tilde{y}} \qquad \tilde{V} = -\frac{\partial\tilde{\psi}}{\partial x}. \tag{9.224}$$

The transformed boundary layer momentum equation finally becomes

$$\left(\tilde{U}\frac{\partial\tilde{U}}{\partial\tilde{x}} + \left(\frac{\partial\tilde{U}}{\partial\tilde{y}}\right)\tilde{V}\right) - \left(\frac{a^2 + \frac{(\gamma-1)}{2}U^2}{a_e^2 + \frac{(\gamma-1)}{2}U_e^2}\right)\tilde{U}_e\frac{d\tilde{U}_e}{d\tilde{x}} - \nu_t\left(\frac{\partial^2\tilde{U}}{\partial\tilde{y}^2}\right) - \frac{1}{\rho_t}\frac{\partial}{\partial\tilde{y}}\left(\tilde{\tau}_{xy}\Big|_{turbulent}\right) \tag{9.225}$$

For an adiabatic wall and $P_r = 1$ the factor in brackets is equal to one. In this case the momentum equation maps exactly to the incompressible form.

$$\left(\tilde{U}\frac{\partial\tilde{U}}{\partial\tilde{x}} + \left(\frac{\partial\tilde{U}}{\partial\tilde{y}}\right)\tilde{V}\right) - \tilde{U}_e\frac{d\tilde{U}_e}{d\tilde{x}} - \nu_t\left(\frac{\partial^2\tilde{U}}{\partial\tilde{y}^2}\right) - \frac{1}{\rho_t}\frac{\partial}{\partial\tilde{y}}\left(\tilde{\tau}_{xy}\Big|_{turbulent}\right) = 0 \tag{9.226}$$

with boundary conditions

$$\tilde{U}(0) = 0 \qquad \tilde{V}(0) = 0 \qquad \tilde{U}(\tilde{\delta}) = \tilde{U}_e \tag{9.227}$$

The implication of (9.226) and (9.227) is that the effects of compressibility on the boundary layer can be almost completely accounted for by the scaling of coordinates presented in (9.195) which is driven in the y direction by the decrease in density near the wall due to heating and in the x direction by the isentropic changes in free stream temperature and boundary layer pressure due to flow acceleration or deceleration imposed by the surrounding potential flow.

Let's use this transformation to relate the skin friction in the compressible case to the incompressible skin friction. The definition of the friction coefficient is

$$\tilde{C}_f = \frac{\tilde{\tau}_w}{(1/2)\rho_t \tilde{U}_e^2} = \frac{\frac{1}{\sigma}\left(\left(\frac{a_t}{a_e}\right)^2 \frac{P_t}{P_e}\right)\tau_w}{(1/2)\left(\frac{\rho_t}{\rho_e}\right)\rho_e\left(\frac{a_t}{a_e}\right)^2 U_e^2} = \frac{1}{\sigma}\frac{\rho_e P_t}{\rho_t P_e}\left(\frac{\tau_w}{(1/2)\rho_e U_e^2}\right) = \frac{1}{\sigma}\frac{T_t}{T_e}C_f \tag{9.228}$$

Recall that for $P_r = 1$ the constant $\sigma = 1$. In terms of the Mach number, the ratio of friction coefficients in the real compressible flow and the virtual incompressible flow is

$$\frac{C_f}{\tilde{C}_f} = \frac{1}{1 + \left(\frac{\gamma - 1}{2}\right)M_e^2}. \tag{9.229}$$

The physical velocity profiles in the compressible flow cannot be determined without solving for the temperature in the boundary layer. Here we will restrict our attention to the laminar, zero pressure gradient, Blasius case, $dU_e/dx = 0$, $\tau_{xy}\big|_{turbulent} = 0$. The temperature equation was integrated earlier to give

$$T = T_t - \frac{1}{2C_p}U^2. \tag{9.230}$$

Equation (9.230) can be expressed as

$$\frac{T}{T_e} = 1 + \left(\frac{\gamma - 1}{2}\right) M_e^2 \left(1 - \left(\frac{U}{U_e}\right)^2\right). \tag{9.231}$$

Using the first relation in (9.18) $U/U_e = \tilde{U}/\tilde{U}_e$, and the equality $\rho T = \rho_e T_e$, equation (9.231) becomes

$$\frac{T}{T_e} = 1 + \left(\frac{\gamma - 1}{2}\right) M_e^2 \left(1 - \left(\frac{\tilde{U}}{\tilde{U}_e}\right)^2\right) = \frac{\rho_e}{\rho}. \tag{9.232}$$

Our goal is to relate the wall normal coordinate in compressible and incompressible flows. From (9.196)

$$dy = \left(\frac{a_t}{a_e}\right)\left(\frac{\rho_t}{\rho_e}\right)\left(\frac{\rho_e}{\rho}\right) d\tilde{y} = \left(\frac{a_t}{a_e}\right)\left(\frac{\rho_t}{\rho_e}\right)\left(1 + \left(\frac{\gamma - 1}{2}\right) M_e^2 \left(1 - \left(\frac{\tilde{U}}{\tilde{U}_e}\right)^2\right)\right) d\tilde{y} \tag{9.233}$$

The spatial similarity variable in the virtual flow is

$$\tilde{\alpha} = \tilde{y}\left(\frac{\tilde{U}_e}{2\nu_t \tilde{x}}\right)^{1/2} \tag{9.234}$$

Now (9.233) becomes

$$dy = \left(\frac{a_t}{a_e}\right)\left(\frac{\rho_t}{\rho_e}\right)\left(\frac{2\nu_t \tilde{x}}{\tilde{U}_e}\right)^{1/2}\left(1 + \left(\frac{\gamma - 1}{2}\right) M_e^2 \left(1 - \left(\frac{\tilde{U}}{\tilde{U}_e}\right)^2\right)\right) d\left(\tilde{y}\left(\frac{\tilde{U}_e}{2\nu_t \tilde{x}}\right)^{1/2}\right) \tag{9.235}$$

and

$$d\left(y\left(\frac{U_e}{2\nu_e x}\right)^{1/2}\right) = \left(\frac{a_t}{a_e}\right)\left(\frac{\rho_t}{\rho_e}\right)\left(\frac{2\nu_t \tilde{x}}{\tilde{U}_e}\right)^{1/2}\left(\frac{U_e}{2\nu_e x}\right)^{1/2}\left(1 + \left(\frac{\gamma - 1}{2}\right) M_e^2 \left(1 - \left(\frac{\tilde{U}}{\tilde{U}_e}\right)^2\right)\right) d\left(\tilde{y}\left(\frac{\tilde{U}_e}{2\nu_t \tilde{x}}\right)^{1/2}\right) \tag{9.236}$$

Rearrange the coefficient on the right hand side of (9.236) using (9.195) and (9.200).

$$\left(\frac{a_t}{a_e}\right)\left(\frac{\rho_t}{\rho_e}\right)\left(\frac{2\nu_t\tilde{x}}{\tilde{U}_e}\frac{U_e}{2\nu_e x}\right)^{1/2} = \left(\frac{a_t}{a_e}\right)\left(\frac{\rho_t}{\rho_e}\right)\left(\frac{\mu_t}{\mu_e}\frac{\rho_e}{\rho_t}\frac{U_e}{\tilde{U}_e}\frac{\tilde{x}}{x}\right)^{1/2} =$$
$$\left(\frac{a_t}{a_e}\right)\left(\frac{\rho_t}{\rho_e}\right)\left(\frac{T_t}{T_e}\frac{\rho_e}{\rho_t}\frac{a_e}{a_t}\frac{P_e}{P_t}\frac{a_e}{a_t}\right)^{1/2} = \left(\frac{\rho_t}{\rho_e}\right)\left(\frac{T_t}{T_e}\frac{\rho_e}{\rho_t}\frac{\rho_e T_e}{\rho_t T_t}\right)^{1/2} = 1 \tag{9.237}$$

Finally.

$$d\alpha = \left(1 + \left(\frac{\gamma-1}{2}\right)M_e^2\left(1 - \left(\frac{\tilde{U}}{\tilde{U}_e}\right)^2\right)\right)d\tilde{\alpha} \tag{9.238}$$

Integrate (9.238). The similarity variables in the real and virtual flows are related by

$$\alpha(\tilde{\alpha}) = \tilde{\alpha} + \left(\frac{\gamma-1}{2}\right)M_e^2\int_0^{\tilde{\alpha}}\left(1 - \left(\frac{\tilde{U}}{\tilde{U}_e}\right)^2\right)d\tilde{\alpha}' \tag{9.239}$$

The velocity ratio, $\tilde{U}/\tilde{U}_e$ is a known function $F_{\tilde{\alpha}}(\tilde{\alpha})$ from the Blasius solution. The outer edge of the incompressible boundary layer is at $\tilde{\alpha}_e = 4.906/\sqrt{2} = 3.469$. The integral of the velocity term in (9.239) is

$$\int_0^{\tilde{\alpha}_e}\left(1 - \left(\frac{\tilde{U}}{\tilde{U}_e}\right)^2\right)d\tilde{\alpha} = 1.67912\,. \tag{9.240}$$

This allows us to determine how the thickness of the compressible layer depends on Mach number. The outer edge of the compressible boundary layer is at

$$\alpha_e = \tilde{\alpha}_e + \left(\frac{\gamma-1}{2}\right)M_e^2\int_0^{\tilde{\alpha}_e}\left(1 - \left(\frac{\tilde{U}}{\tilde{U}_e}\right)^2\right)d\tilde{\alpha} = \tag{9.241}$$
$$\alpha_e = 3.469 + 1.67912\left(\frac{\gamma-1}{2}\right)M_e^2$$

The thickness of the compressible layer grows rapidly with Mach number. Knowing $\alpha(\tilde{\alpha})$ enables the temperature and density of the compressible layer to be determined.

$$\frac{T(\alpha(\tilde{\alpha}))}{T_e} = \frac{\rho_e}{\rho(\alpha(\tilde{\alpha}))} = 1 + \left(\frac{\gamma - 1}{2}\right) M_e^2 \left(1 - \left(\frac{\tilde{U}(\tilde{\alpha})}{\tilde{U}_e}\right)^2\right) \tag{9.242}$$

Numerically determined solutions for the velocity profile at several Mach numbers are shown below.

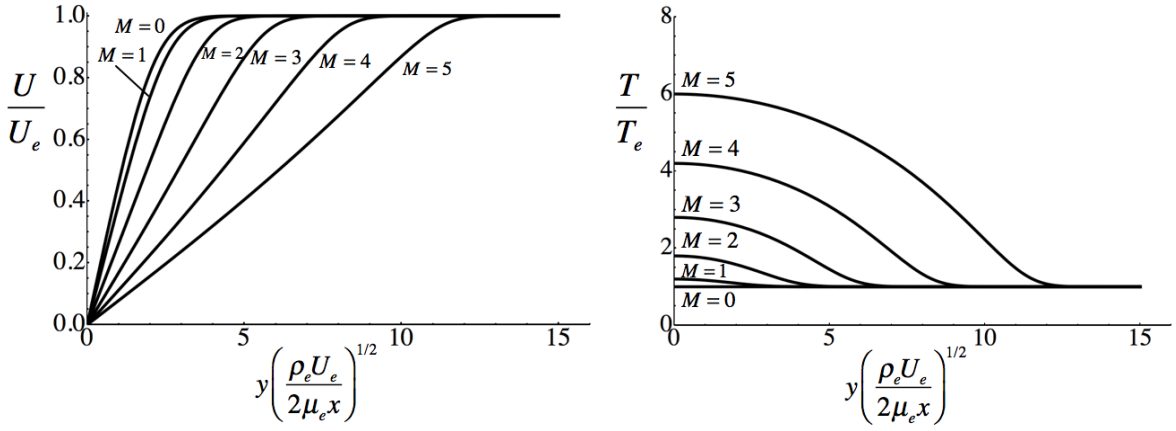

Figure 9.24 Compressible boundary layer profiles on an adiabatic plate for $P_r = 1$, *viscosity exponent* $\omega = 1$, *and* $\gamma = 1.4$.

The compressible layer is considerably thicker than the incompressible layer due to the high temperature and low density near the wall caused by the deceleration of the flow.

9.11 TURBULENT BOUNDARY LAYERS

As the Reynolds number increases along the plate a point is reached where the laminar boundary layer begins to be unstable to small disturbances. A complex series of events occurs by which the flow becomes turbulent characterized by very rapid mixing of momentum in the transverse direction. As a result the velocity profile becomes much fuller and the velocity gradient near the wall becomes much steeper compared to the velocity gradient that would have occurred if the layer had remained laminar. The friction at the wall is also correspondingly much larger and the growth rate of the boundary layer is much faster as suggested schematically in Figure 9.25 below.

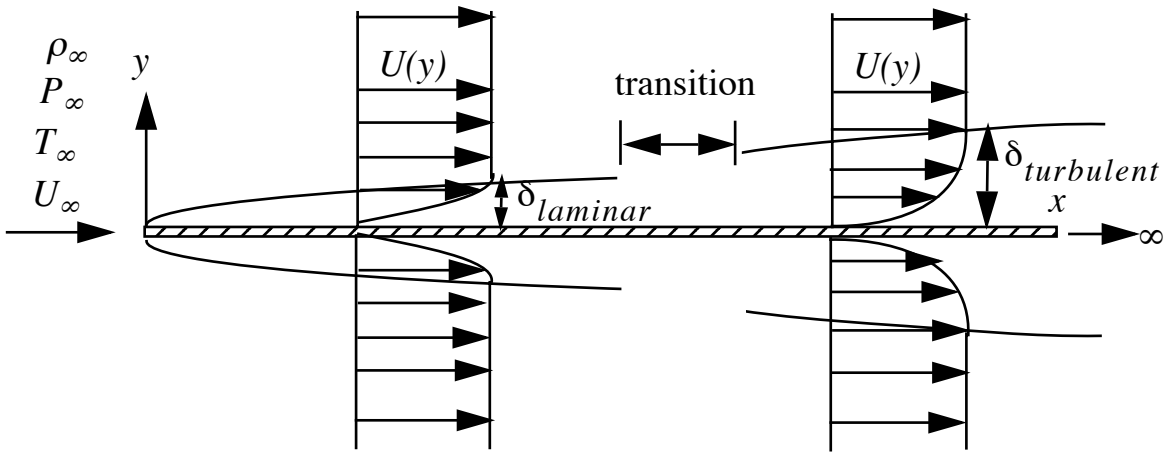

Figure 9.25 Sketch of boundary layer growth in the laminar and turbulent regions.

There is no ab initio theory for the Reynolds shearing stress in a turbulent boundary layer and so there is no fundamental theory for the velocity profile, boundary layer thickness or skin friction. A reasonable and commonly used impirical formula for the thickness of an incompressible turbulent boundary layer is

$$\frac{\delta}{x} = \frac{0.37}{R_{ex}^{1/5}}. \tag{9.243}$$

There is no theoretical reason to assume that the thickness of a turbulent boundary layer grows according to a power law as there is in the laminar case. A relation that applies over a wider range of Reynolds number than (9.243) is Hansen's formula

$$\frac{\delta}{x} = \frac{0.14}{ln(R_{ex})} G(Ln(R_{ex})) \tag{9.244}$$

Where G is a very slowly changing function of the Reynolds number with an asymptotic value of one at $Ln((R_{ex}) \rightarrow \infty)$. In the Reynolds number range $10^5 < R_e < 10^6$, $G = 1.5$.

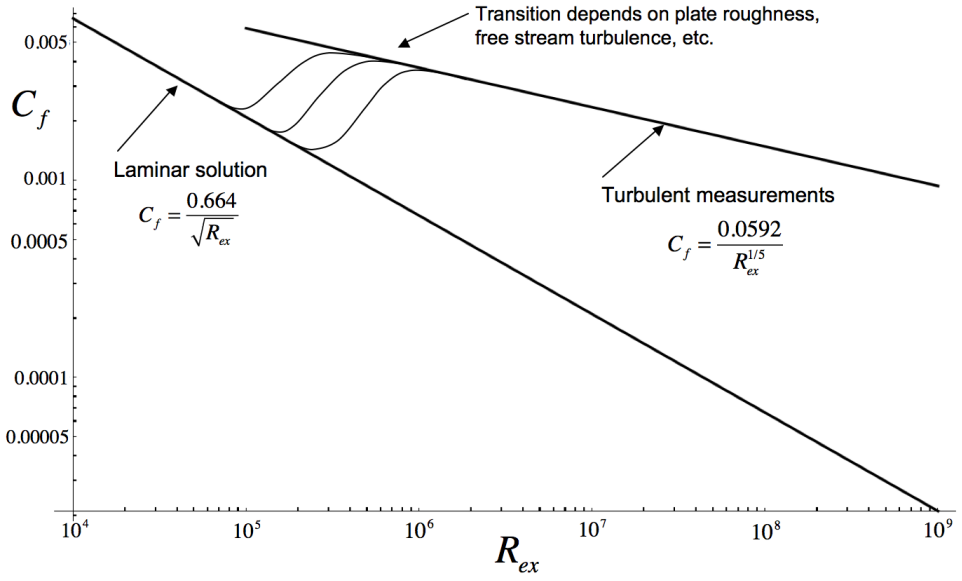

Figure 9.26 Friction coefficient for incompressible flow on a flat plate.

The critical Reynolds number for transition is generally taken to be 5×10^5 although in reality transition is affected by a wide variety of flow phenomena including such things as plate roughness, free stream turbulence, compressibility and the presence of acoustic noise in the free stream. Figure 9.26 is intended to illustrate this idea with the theoretical laminar and impirical turbulent skin friction lines connected by a several curves reflecting the disturbance environment of a particular flow. In the transition zone the physical wall shear stress can actually increase in the x direction due to the rapid filling out of the velocity profile as the turbulence develops.

9.11.1 THE INCOMPRESSIBLE TURBULENT BOUNDARY LAYER VELOCITY PROFILE

A commonly used impirical form of the velocity profile for a turbulent boundary layer is the so-called $1/7th$ power law.

$$\frac{U}{U_e} = \left(\frac{y}{\delta}\right)^{1/7} \tag{9.245}$$

This profile can be useful in a limited range of Reynolds numbers but it fails to capture one of the most important features of the turbulent boundary layer which is that the actual shape of the velocity profile depends on the Reynolds number. In contrast, the Blasius profile shape is completely independent of Reynolds number. Only the thickness changes with Reynolds number.

While there is no good theory for the velocity profile in a turbulent boundary, there is a very good correlation that accurately reflects certain fundamental flow properties and can be used to analyze and compare flows at different Reynolds numbers.

The first thing to know is that the flow near the wall, when properly normalized, has a universal shape that is independent of the parameters that govern the outer flow. The idea is to normalize the velocity near the wall by the so-called friction velocity

$$u^* = \sqrt{\frac{\tau_w}{\rho}} \qquad \tau_w = \mu \left.\frac{\partial U}{\partial y}\right|_{y=0} \tag{9.246}$$

This leads to the definition of dimensionless wall variables.

$$y^+ = \frac{yu^*}{\nu} \qquad U^+ = \frac{U}{u^*} \tag{9.247}$$

The thickness of the boundary layer in wall units is

$$\delta^+ = \frac{\delta u^*}{\nu} \tag{9.248}$$

If we use the impirical formulas for thickness and skin friction described above then

$$\frac{u^*}{U_e} = \left(\frac{\tau_w}{\rho U_e^2}\right)^{1/2} = \left(\frac{C_f}{2}\right)^{1/2} = \left(\frac{0.0592}{2R_{ex}^{1/5}}\right)^{1/2} = \frac{0.172}{R_{ex}^{1/10}} \tag{9.249}$$

and

$$\delta^+ = \frac{\delta}{x}\frac{u*}{U_e}\frac{U_e x}{\nu} = \left(\frac{0.37}{R_{ex}^{1/5}}\right)\left(\frac{0.172}{R_{ex}^{1/10}}\right)R_{ex} = 0.0636R_{ex}^{7/10} \tag{9.250}$$

In other words, once R_{ex} is known most of the important properties of the boundary layer are known. A typical velocity profile is shown below. I have chosen a relatively low Reynolds number so that the flow near the wall can be seen at a reasonable scale.

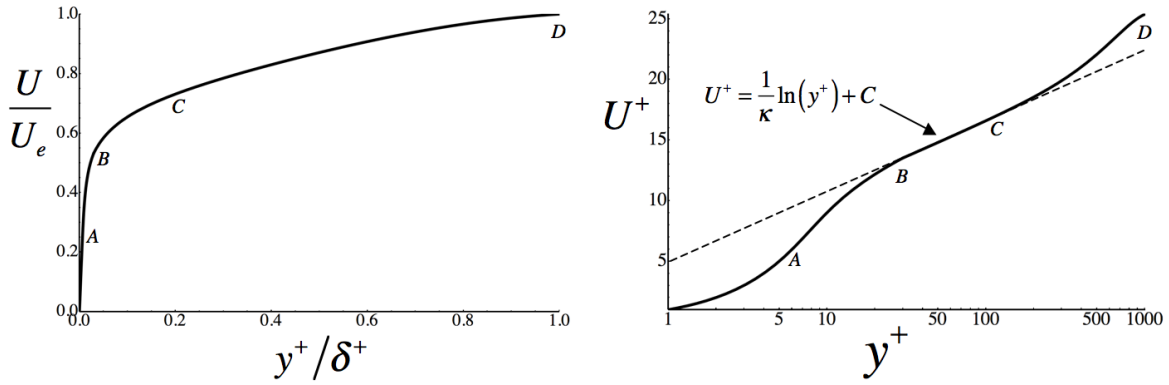

Figure 9.27 Turbulent boundary layer velocity profile in linear and log-linear coordinates. The Reynolds number is $R_{ex} = 10^6$

The boundary layer is generally thought of as comprising several layers and these are indicated in Figure 9.27. Usually they are delineated in terms of wall variables.

Viscous sublayer - Wall to A, $0 \le y^+ < 7$. In this region closest to the wall the velocity profile is linear.

$$U^+ = y^+ \tag{9.251}$$

Buffer layer - A to B, $7 \le y^+ < 30$. Several alternative formulations are used to approximate the velocity in this region. An implicit relation that works reasonably well all the way to the wall is

$$y^+ = U^+ + e^{-\kappa C}\left(e^{\kappa U^+} - 1 - \kappa U^+ - \frac{1}{2}(\kappa U^+)^2 - \frac{1}{6}(\kappa U^+)^3 - \frac{1}{24}(\kappa U^+)^4\right) \tag{9.252}$$

Logarithmic and outer layer - B to C to D $30 \le y^+ < \delta^+$. An impirical formula that works well and includes the effect of pressure gradient is

$$U^+ = \frac{1}{\kappa} ln(y^+) + C + 2\frac{\Pi(x)}{\kappa} Sin^2\left(\frac{\pi y^+}{2\delta^+}\right) \tag{9.253}$$

The slope of the profile in the logarithmic region is inversely proportional to the Karman constant κ which is generally taken to be $\kappa = 0.4$ and is viewed as a universal constant of turbulent flows. However modelers of meteorological flows such as the atmospheric boundary layer have deduced values of κ as low as 0.35 while recent experiments in very high Reynolds number pipe flow at Princeton have suggested values as high as 0.436.

The constant C depends on the wall roughness. If k_s is a measure of the height of roughness elements at the wall one can define $R_{es} = u^* k_s/\nu$ as a roughness Reynolds number. The wall is considered hydraulically smooth if $R_{es} < 3$ and hydraulically rough if $R_{es} > 100$. For a hydraulically smooth wall $C = 5.1$ in (9.253) and increases with increasing R_{es}. The function $\Pi(x)$ is determined by the pressure gradient and layer Reynolds number. For $dP_e/dx = 0$, $\Pi = 0.62$. The logarithmic term in (9.253) is remakably robust in the presence of pressure gradients and roughness. The constant κ hardly changes at all with roughness.

The Sin^2 term in (9.253) is called the wake function because of the vaguely wake like shape of the outer velocity profile. Something to notice is that the velocity profile (9.253) is not valid beyond $y^+ = \delta^+$ and the velocity profile has a small but finite slope at $y^+ = \delta^+$ because of the logarithmic term.

Figure 9.28 compares turbulent boundary layer profiles at various Reynolds numbers. The effect of Reynolds number on the flow expressed in wall variables is felt through the value of δ^+ in the wake function term in (9.253). In Figure 9.28 there is a slight mismatch between (9.252) and (9.253) at the outer edge of the buffer

layer at a Reynolds number of 10^5. This is because a turbulent boundary layer can hardly exist at such a low Reynolds number and the functions (9.252) and (9.253) which have been developed from boundary layer data were not designed to fit this case.

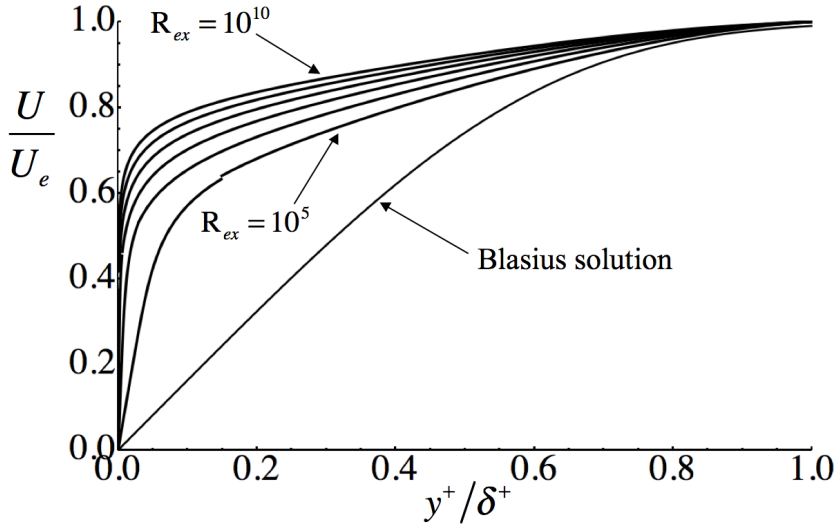

Figure 9.28 Incompressible turbulent boundary layer velocity profiles at several Reynolds numbers compared to the Blasius solution for a laminar boundary layer.

The most remarkable feature of the turbulent boundary layer is the logarithmic region B to C governed by the so-called universal law of the wall. In this region the wake function is negligible and the velocity profile has the same shape regardless of the Reynolds number. The shape remains the same even in the presence of a pressure gradient which is remarkable in view of the sensitivity of the shape of the laminar velocity profile to pressure gradient. If the plate is rough the main effect is to increase the value of the constant C while preserving the logarithmic shape and the slope $1/\kappa$.

According to (9.250) δ^+ increases fairly rapidly with Reynolds number and this leads to an increasingly full velocity profile. At high Reynolds numbers the viscous sublayer becomes extremely thin. At high Reynolds number it is very difficult to make direct measurements of the linear part of the velocity profile to

determine skin friction. Fortunately the skin friction can be determined using measurements in the much more accessible logarithmic region by utilizing the law of the wall.

$$\frac{U}{U^*} = \frac{1}{\kappa} ln\left(\frac{yU^*}{\nu}\right) + C \tag{9.254}$$

Measurements of U versus y in region B-C can be used to determine U^* and hence C_f. The friction coefficient in the compressible case can be estimated using (9.229).

9.12 TRANSFORMATION BETWEEN FLAT PLATE AND CURVED WALL BOUNDARY LAYERS

One of the consequences of the boundary layer approximation is that the solution for the flow on a flat plate with a variable free stream velocity can be transformed directly to the solution on a curved wall with the same free stream velocity function. Once again the boundary layer equations are

$$\begin{aligned} \frac{\partial \rho U}{\partial x} + \frac{\partial \rho V}{\partial y} &= 0 \\ \rho U \frac{\partial U}{\partial x} + \rho V \frac{\partial U}{\partial y} + \frac{dP_e}{dx} - \frac{\partial \tau_{xy}}{\partial y} &= 0 \\ \rho U C_p \frac{\partial T}{\partial x} + \rho V C_p \frac{\partial T}{\partial y} - U \frac{dP_e}{dx} + \frac{\partial Q_y}{\partial y} - \tau_{xy} \frac{\partial U}{\partial y} &= 0 \end{aligned} \tag{9.255}$$

where τ_{xy} includes both laminar and turbulent components of shearing stress and Q_y includes laminar and turbulent componenst of heat flux. The transformation of variables between the flat plate and curved wall is.

$$
\begin{aligned}
\tilde{x} &= x \\
\tilde{y} &= y + g(x) \\
\tilde{U}(\tilde{x}, \tilde{y}) &= U(x, y) \\
\tilde{V}(\tilde{x}, \tilde{y}) &= V(x, y) + U(x, y)\frac{dg(x)}{dx} \\
\tilde{\rho}(\tilde{x}, \tilde{y}) &= \rho(x, y) \\
\tilde{\tau}_{xy}(\tilde{x}, \tilde{y}) &= \tau_{xy}(x, y) \\
\tilde{Q}_y(\tilde{x}, \tilde{y}) &= Q_y(x, y) \\
P_e(\tilde{x}) &= P_e(x)
\end{aligned}
\tag{9.256}
$$

The transformation (9.256) generates the transformation of derivatives using the chain rule.

$$
\begin{aligned}
\frac{\partial \tilde{U}}{\partial \tilde{x}} &= \frac{\partial U}{\partial x} - \frac{dg}{dx}\frac{\partial U}{\partial y} & \frac{\partial \tilde{\rho}}{\partial \tilde{y}} &= \frac{\partial \rho}{\partial y} \\
\frac{\partial \tilde{U}}{\partial \tilde{y}} &= \frac{\partial U}{\partial y} & \frac{\partial \tilde{T}}{\partial \tilde{x}} &= \frac{\partial T}{\partial x} - \frac{dg}{dx}\frac{\partial T}{\partial y} \\
\frac{\partial^2 \tilde{U}}{\partial \tilde{y}^2} &= \frac{\partial^2 U}{\partial y^2} & \frac{\partial \tilde{T}}{\partial \tilde{y}} &= \frac{\partial T}{\partial y} \\
\frac{\partial \tilde{V}}{\partial \tilde{y}} &= \frac{\partial V}{\partial y} + \frac{dg}{dx}\frac{\partial U}{\partial y} & \frac{\partial \tilde{Q}_y}{\partial \tilde{y}} &= \frac{\partial Q_y}{\partial y} \\
\frac{\partial \tilde{\rho}}{\partial \tilde{x}} &= \frac{\partial \rho}{\partial x} - \frac{dg}{dx}\frac{\partial \rho}{\partial y} & \frac{\partial \tilde{\tau}_{xy}(\tilde{x}, \tilde{y})}{\partial \tilde{y}} &= \frac{\partial \tau_{xy}(x, y)}{\partial y}
\end{aligned}
\tag{9.257}
$$

The transformation (9.257) and its extension to derivatives (9.257) maps (9.255) to itself.

$$
\begin{aligned}
\frac{\partial \tilde{\rho}\tilde{U}}{\partial \tilde{x}} + \frac{\partial \tilde{\rho}\tilde{V}}{\partial \tilde{y}} &= \frac{\partial \rho U}{\partial x} + \frac{\partial \rho V}{\partial y} = 0 \\
\tilde{\rho}\tilde{U}\frac{\partial \tilde{U}}{\partial \tilde{x}} + \tilde{\rho}\tilde{V}\frac{\partial \tilde{U}}{\partial \tilde{y}} + \frac{d\tilde{P}_e}{d\tilde{x}} - \frac{\partial \tilde{\tau}_{xy}}{\partial \tilde{y}} &= \rho U\frac{\partial U}{\partial x} + \rho V\frac{\partial U}{\partial y} + \frac{dP_e}{dx} - \frac{\partial \tau_{xy}}{\partial y} = 0 \\
\tilde{\rho}\tilde{U}C_p\frac{\partial \tilde{T}}{\partial \tilde{x}} + \tilde{\rho}\tilde{V}C_p\frac{\partial \tilde{T}}{\partial \tilde{y}} - \tilde{U}\frac{d\tilde{P}_e}{d\tilde{x}} + \frac{\partial \tilde{Q}_y}{\partial \tilde{y}} - \tilde{\tau}_{xy}\frac{\partial \tilde{U}}{\partial \tilde{y}} &= \\
\rho U C_p\frac{\partial T}{\partial x} + \rho V C_p\frac{\partial T}{\partial y} - U\frac{dP_e}{dx} + \frac{\partial Q_y}{\partial y} - \tau_{xy}\frac{\partial U}{\partial \tilde{y}} &= 0
\end{aligned}
\tag{9.258}
$$

In principle the function $g(x)$ added to the y coordinate is arbitrary, but in practice $g(x)$ is restricted to be smooth and slowly varying so as not to violate the boundary layer approximation.

It is the absence of the derivative $\partial V / \partial x$ from (9.255) that enables the transformation (9.256) and (9.257) to reproduce the same equations in the new coordinates. The figure below illustrates the idea.

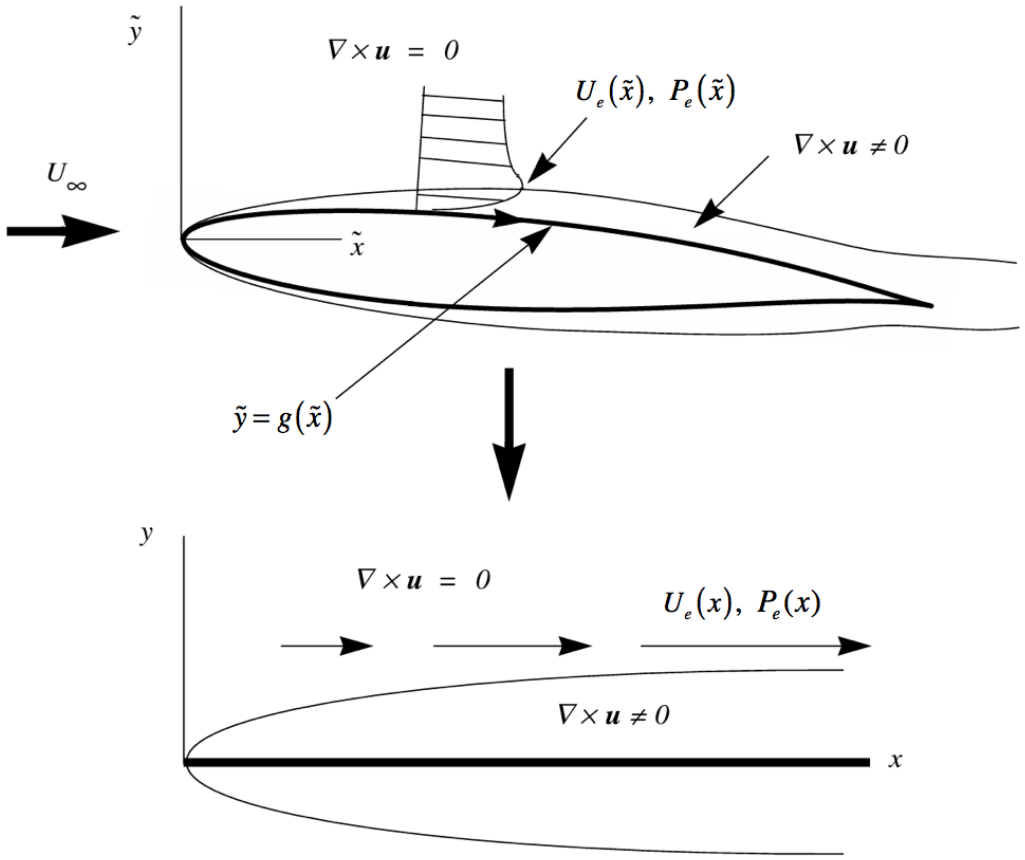

Figure 9.29 Mapping of the boundary layer developing over an airfoil to the boundary layer on a flat plate with a pressure gradient.

The function $g(\tilde{x})$ defines the surface of the airfoil in the Cartesian coordinates $(\tilde{x}, \tilde{y})$. The flow at a given $\tilde{x}$ distance from the leading edge and a distance $\tilde{y} - g(\tilde{x})$ above the surface of the airfoil is mapped to the same position in the boundary layer on a flat plate with the same free stream flow velocity

$\tilde{U}_e(\tilde{x}) = U_e(x)$. The main restriction on $g(\tilde{x})$ is that it vary slowly enough so that the boundary layer does not approach separation and so that the approximation $\tilde{x} \cong x$ remains valid.

The exponential decay of the vorticity at the edge of the boundary layer described earlier, together with this simple invariance of the boundary layer equations enables boundary layer theory to be applied to a wide variety of slender body shapes creating one of the most powerful tools in fluid mechanics.

An iterative algorithm can be used to determine the viscous flow over a complex shape such as the airfoil shown in Figure 9.29. The procedure is

1) Solve for the potential flow over the airfoil.

2) Use the potential flow velocity at the airfoil surface as the $U_e(x)$ for a boundary layer calculation beginning at the leading edge.

3) Determine the displacement thickness of the boundary layer and use the data to define a new airfoil shape. Repeat the potential flow calculation using the new airfoil shape to determine a new $U_e(x)$.

4) Using the new $U_e(x)$ repeat the boundary layer calculation.

A few iterations of this viscous-inviscid interaction procedure will converge to an accurate solution for the viscous, compressible flow over the airfoil.

9.13 PROBLEMS

Problem 1 - The figure below depicts Couette flow of an ideal gas between two infinite parallel. The lower wall is adiabatic.

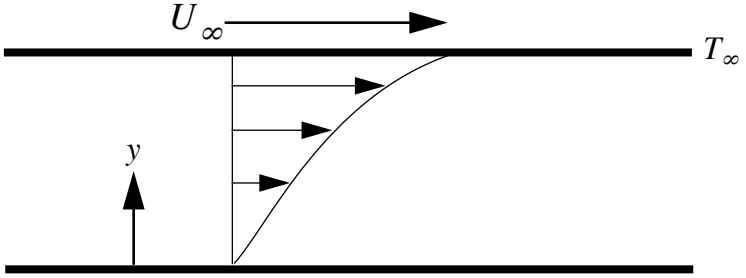

Determine the entropy difference between the lower and upper walls.

Problem 2 - The figure below depicts Couette flow of helium gas between two infinite parallel walls spaced 1 cm apart. The lower wall is adiabatic and the speed of the upper wall is 400 meters/sec. The temperature of the upper wall is 300K.

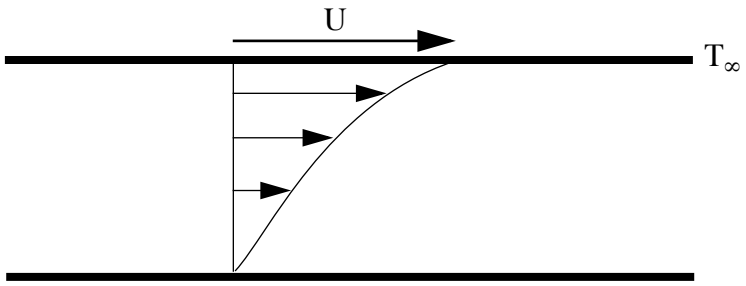

Assume the viscosity depends linearly on temperature.

$$\mu / \mu_\infty = T / T_\infty . \tag{9.259}$$

Set up and solve the compressible flow equations for this simple flow. Note that the flow is assumed to be steady and all flow variables depend only on the coordinate normal to the wall.

1) Determine the speed of sound at the upper wall.

2) Determine the temperature of the lower wall.

3) Determine the shear stress.

4) Is there work done on the flow? How much?

5) Determine the heat flux through the upper wall.

6) Sketch the distribution of stagnation temperature across the channel.

7) Sketch the distribution of entropy across the channel.

Problem 3 - The figure below depicts Couette flow of a gas between two infinite parallel walls spaced a distance d apart. The lower wall is adiabatic. The reference Mach number is $M_\infty = U_\infty / \sqrt{\gamma R T_\infty}$. The viscosity is assumed to depend linearly on temperature $\mu / \mu_\infty = T / T_\infty$ and the reference Reynolds number is $R_e = \rho_\infty U_\infty d / \mu_\infty$.

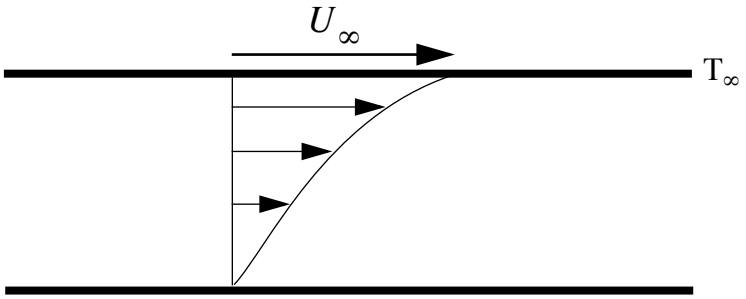

Sketch how the friction coefficient C_f depends on U_∞. At what Mach number is the friction coefficient an extremum? Is it a maximum or a minimum? Express your answer in terms of γ and the Prandtl number. What are the values for helium and air?

Problem 4 - The figure below shows the unsteady flow produced by a flat plate set into motion impulsively at velocity U_∞.

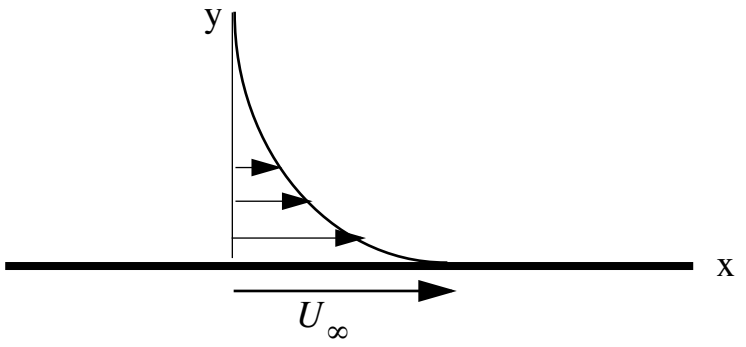

The plate extends to infinity in both directions and the flow is perfectly parallel. Simplify the compressible flow equations. Solve for the velocity and vorticity in the incompressible case.

Problem 5 - In the discussion of boundary layers we defined several definitions of the thickness. How would you define a thickness based on the vorticity distribution? What might be the advantage of such a definition?

Problem 6 - Use the Howarth-Stewartson transformation to generate the velocity and temperature profiles in a laminar, compressible, zero pressure-gradient boundary layer at a free stream Mach number $M_\infty = 8$.